

ADA 035298

REPORT NO. FAA-RD-76-216

12

ILS GLIDE SLOPE  
PERFORMANCE PREDICTION  
MULTIPATH SCATTERING

S. Morin  
D. Newsom  
M. Scotto

U.S. Department of Transportation  
Transportation Systems Center  
Kendall Square  
Cambridge MA 02142



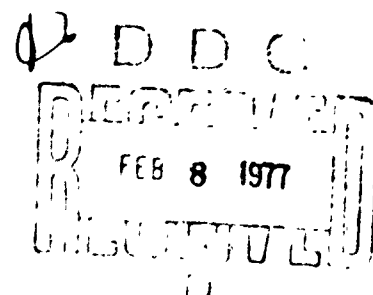
DECEMBER 1976

FINAL REPORT

DOCUMENT IS AVAILABLE TO THE U.S. PUBLIC  
THROUGH THE NATIONAL TECHNICAL  
INFORMATION SERVICE, SPRINGFIELD,  
VIRGINIA 22161

Prepared for

U.S. DEPARTMENT OF TRANSPORTATION  
FEDERAL AVIATION ADMINISTRATION  
Systems Research and Development Service  
Washington DC 20591



**NOTICE**

This document is disseminated under the sponsorship of the Department of Transportation in the interest of information exchange. The United States Government assumes no liability for its contents or use thereof.

Technical Report Documentation Page

1. Report No. 18 FAA-RD-76-216	2. Government Accession No.	3. Recipient's Catalog No.
4. Title and Subtitle 6 ILS GLIDE SLOPE PERFORMANCE PREDICTION MULTIPATH SCATTERING	5. Report Date 11 Dec 1976	6. Performance and/or Evaluation Code 14
7. Author(s) 10 S. Morin, D. Newsom, M. Scotto	8. Performance and/or Evaluation Report No. TSC-FAA-76-16	9. Work Unit No. (YRALS) FA687/R7143
12. Sponsoring Agency Name and Address U.S. Department of Transportation Federal Aviation Administration Systems Research & Development Service Washington DC 20591	11. Contract or Grant No.	13. Report Period Final Report July 1975-March 1976
15. Supplementary Notes 128 pp.	14. Sponsoring Agency Code ARD-741	
16. Abstract A mathematical model has been developed which predicts the performance of ILS glide slope systems subject to multipath scattering and the effects of irregular terrain contours. The model is discussed in detail and then applied to a test case for purposes of illustration. A complete listing of all computer programs has been appended to the report. A users' manual has been prepared under separate cover.		
17. Key Words ILS Derogation CDI Glide Slope	18. Distribution Statement DOCUMENT IS AVAILABLE TO THE U.S. PUBLIC THROUGH THE NATIONAL TECHNICAL INFORMATION SERVICE, SPRINGFIELD, VIRGINIA 22161	
19. Security Classif. (of this report) Unclassified	20. Security Classif. (of this page) Unclassified	21. No. of Pages 82
22. Price		

407082

16

## PREFACE

The work presented in this report has been sponsored by the Federal Aviation Administration as part of a program to provide navigational aids for the safe landing of aircraft. The program has been concerned with the application of instrument landing aids, and in particular the development of models to predict the performance of localizer and glide slope antenna systems. The present report is concerned with the glide slope portion of instrument landing system, and the effects of airport topography on its performance.

**SECTION 7**

<b>WATER SECTION</b>	<input checked="" type="checkbox"/>
<b>SOIL SECTION</b>	<input type="checkbox"/>
<b>ROCK SECTION</b>	<input type="checkbox"/>

**NOTE:** The following information is required for all sections.

1. Name of the section  
2. Date of the section  
3. Location of the section  
4. Name of the person who made the section  
5. Name of the person who checked the section  
6. Name of the person who approved the section  
7. Name of the person who submitted the section

A

DDC  
RECEIVED  
FEB 8 1977  
RECEIVED  
D

# METRIC CONVERSION FACTORS

Approximate Conversions to Metric Measures				Approximate Conversions from Metric Measures			
Symbol	When You Know	Multiply by	To Find	Symbol	When You Know	Multiply by	To Find
<b>LENGTH</b>				<b>LENGTH</b>			
m	meters	1	meters	mm	millimeters	0.001	meters
cm	centimeters	0.01	meters	cm	centimeters	0.01	meters
dm	decimeters	0.1	meters	m	meters	1	meters
km	kilometers	1,000	meters	km	kilometers	1,000	meters
<b>AREA</b>				<b>AREA</b>			
m <sup>2</sup>	square meters	1	square meters	m <sup>2</sup>	square meters	1	square meters
cm <sup>2</sup>	square centimeters	0.0001	square meters	cm <sup>2</sup>	square centimeters	0.0001	square meters
dm <sup>2</sup>	square decimeters	0.01	square meters	dm <sup>2</sup>	square decimeters	0.01	square meters
ha	hectares	10,000	square meters	ha	hectares	10,000	square meters
<b>MASS (weight)</b>				<b>MASS (weight)</b>			
g	grams	0.001	kilograms	g	grams	0.001	kilograms
kg	kilograms	1	kilograms	kg	kilograms	1	kilograms
lb	pounds	0.45	kilograms	lb	pounds	0.45	kilograms
oz	ounces	0.028	kilograms	oz	ounces	0.028	kilograms
<b>VOLUME</b>				<b>VOLUME</b>			
m <sup>3</sup>	cubic meters	1	cubic meters	m <sup>3</sup>	cubic meters	1	cubic meters
cm <sup>3</sup>	cubic centimeters	0.000001	cubic meters	cm <sup>3</sup>	cubic centimeters	0.000001	cubic meters
dm <sup>3</sup>	cubic decimeters	0.001	cubic meters	dm <sup>3</sup>	cubic decimeters	0.001	cubic meters
l	liters	0.001	cubic meters	l	liters	0.001	cubic meters
gal	gallons	0.0038	cubic meters	gal	gallons	0.0038	cubic meters
cu ft	cubic feet	0.028	cubic meters	cu ft	cubic feet	0.028	cubic meters
cu yd	cubic yards	0.76	cubic meters	cu yd	cubic yards	0.76	cubic meters
<b>TEMPERATURE (exact)</b>				<b>TEMPERATURE (exact)</b>			
°C	Celsius temperature	5/9 (°F minus 32)	Fahrenheit temperature	°C	Celsius temperature	5/9 (°F minus 32)	Fahrenheit temperature
°F	Fahrenheit temperature	9/5 (°C plus 32)	Celsius temperature	°F	Fahrenheit temperature	9/5 (°C plus 32)	Celsius temperature

## CONTENTS

<u>Section</u>	<u>Page</u>
1. INTRODUCTION.....	1
2. BASIC THEORY.....	1
Part A.....	1
Part B.....	17
3. NUMERICAL RESULTS.....	19

## ILLUSTRATIONS

<u>Figure</u>	<u>Page</u>
1. TYPICAL GEOMETRY FOR MULTIPATH SCATTERING.....	2
2. REPRESENTATION OF RECTANGULAR FACET.....	9
3. TYPICAL PROFILE OF ONE-DIMENSIONAL TERRAIN VARIATION.....	18
4. OVERVIEW OF A MULTIPATH CONFIGURATION.....	24
5. NULL REFERENCE ARRAY, FLYABILITY RUN.....	25
6. SIDEBAND REFERENCE ARRAY, FLYABILITY RUN.....	26
7. CAPTURE EFFECT ARRAY, FLYABILITY RUN.....	27

## 1. INTRODUCTION

A mathematical model has been developed for predicting the performance of image-type glide slope arrays. The basic theory is developed in the following section of this report. In Part A of that section a model of the glide slope multipath problem is developed while in Part B the techniques for dealing with irregular terrain profiles are outlined. In the final section of the report some illustrative numerical results are presented.

## 2. BASIC THEORY

### PART A

The presence in the airport environment of such large man-made structures as aircraft hangars as well as such natural terrain features as hillsides can lead to glide slope course derogation through multipath scattering. We begin our treatment of glide slope siting problems by developing a model for predicting the amount of such multipath derogation. A typical situation is depicted in Figure 1.

The touchdown point on the centerline of the runway opposite the glide slope array is chosen as the origin of coordinates 0. The z-axis is chosen to be the vertical axis passing through the origin 0, while the x-and y-axes are parallel to and perpendicular to the centerline, respectively. The positive z-axis points out of the page (Figure 1). The ground plane is assumed to be perfectly conducting. Consequently, any deviations from nominal glide slope performance are attributable to the multipath scattering produced by the various structures (both natural and man-made). For simplicity, we will assume that all such structures are perfectly conducting.

In the situation depicted in Figure 1, the scatterer (perhaps a small hill) is illuminated by the glide slope array and scatters

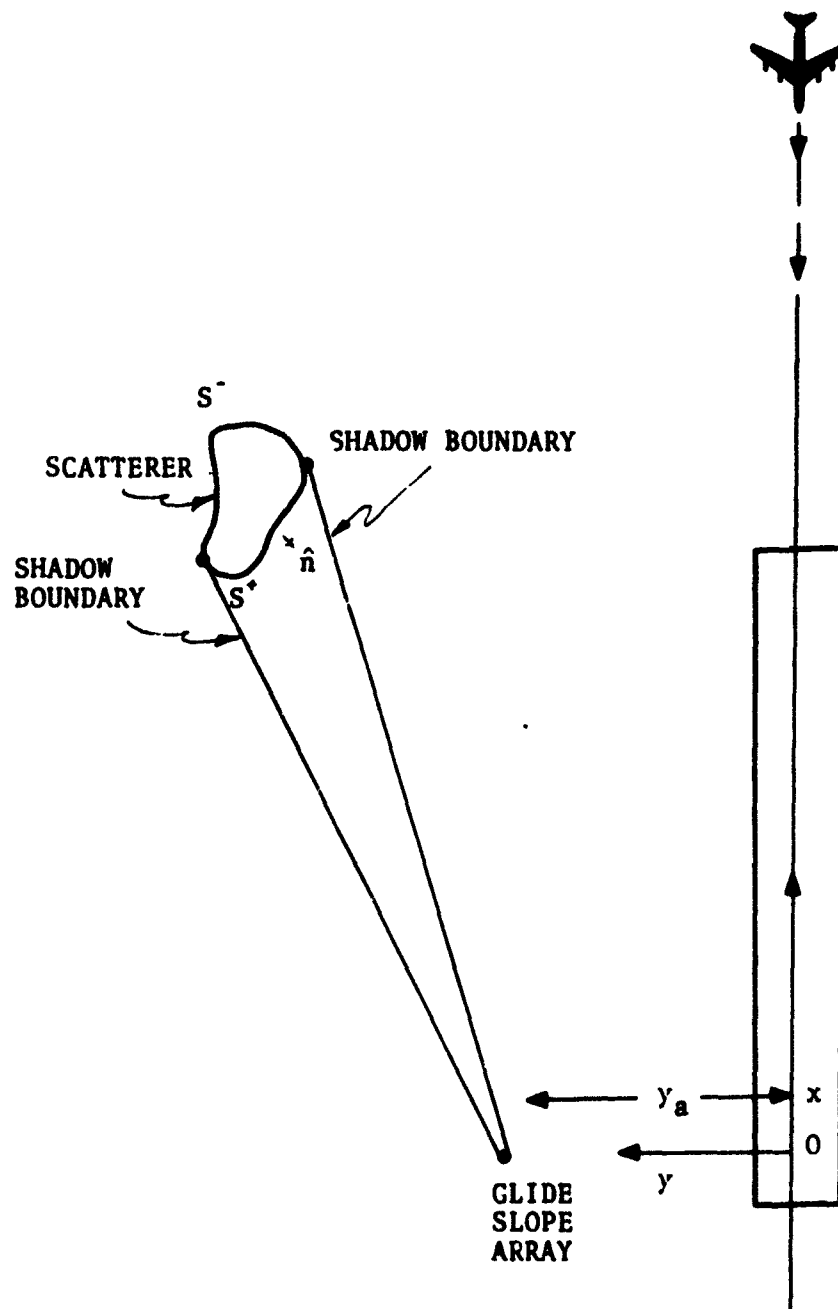


FIGURE 1. TYPICAL GEOMETRY FOR MULTIPATH SCATTERING



some of this signal back into the path of the approaching aircraft. We now proceed to calculate mathematical expressions for these scattered fields at the receiver. For convenience, we will work with magnetic field intensities.

For a perfect conductor, the surface current density  $\vec{K}$  is given by:

$$\vec{K} = \hat{n} \times \vec{H}, \quad (1)$$

where  $\hat{n}$  is the local unit normal vector pointing out of the scattering surface and  $\vec{H}$  is the total magnetic field,

$$\vec{H} = \vec{H}_i + \vec{H}_s, \quad (2)$$

where  $\vec{H}_i$  is the incident and  $\vec{H}_s$  the scattered field on the surface of the scattering structure. In terms of the surface current density  $\vec{K}$ , the scattered field  $\vec{H}_s$  at the receiver is given by the following surface integral:

$$\vec{H}_s(\vec{r}_1) = \frac{1}{4\pi} \int_S [\vec{K}(\vec{r}) \times \nabla G(\vec{r}_1, \vec{r})] ds \quad (3)$$

In Equation (3), the vectors  $\vec{r}_1$  and  $\vec{r}$  denote, respectively, the position vector of the receiver and the position vector of some arbitrary source point on the surface of the scatterer relative to the origin of coordinates 0. The two-point Green's function  $G(\vec{r}_1, \vec{r})$  is given by:

$$G(\vec{r}_1, \vec{r}) = \frac{e^{ik|\vec{r}_1 - \vec{r}|}}{|\vec{r}_1 - \vec{r}|} \quad (4)$$

where  $k = 2\pi/\lambda$  and  $\lambda$  is the wavelength of the incident radiation. The integral is taken over the surface  $S$  of the scatterer.

We will adopt here the single scattering, physical optics approximation for the current density  $\vec{K}$ . Specifically, we will assume that on those portions of the scattering surface not directly illuminated by the glide slope array,  $\vec{K}$  is identically zero and

that on the directly illuminated portions of the scattering surface,  $K$  is proportional to twice the tangential component of the incident magnetic field:

$$\vec{K} \equiv 0 \text{ on } S_- \quad (5)$$

$$\vec{K} = 2 (\hat{n} \times \vec{H}_i) \text{ on } S_+ \quad (6)$$

where  $S_+$  and  $S_-$  denote, respectively, the illuminated and unilluminated portions of the scattering surface  $S$  (see Figure 1). For the current distribution defined by Equations (5) and (6), Equation (3) becomes.

$$\vec{H}_s(\vec{r}_1) = -\frac{1}{2\pi} \int_{S_+} [\hat{n}(\vec{r}) \times \vec{H}_i(\vec{r})] \times \vec{\nabla} G(\vec{r}_1, \vec{r}) ds. \quad (7)$$

The physical optics scattering model represented by equation (7) is based upon the existence of a sharp shadow boundary on the surface of the scattering structure. This assumption ignores such phenomena multiple reflections, surface waves, and diffraction but should provide reasonably accurate results as long as the surface features of the scattering structure do not vary greatly over dimensions which are small compared to the wavelength  $\lambda$  (about 3 feet at glide slope frequencies).

In principle, the solution to the problem at hand requires only that the magnet field  $H_i$  be determined. For simplicity, we will assume that the glide slope array is made up of electrically short dipoles. With this assumption, we in effect approximate by a cosine distribution the actual azimuthal pattern of the half-wave dipoles which make up glide slope arrays. This approximation should not be too restrictive and it does considerably expedite our calculations. Let  $(0, y_a, h)$  denote the  $x$ ,  $y$ , and  $z$  coordinates respectively of a typical dipole in the array and let  $(x, y, z)$  denote the coordinates of a point  $\vec{r}$  at which we wish to know the magnetic field intensity  $H_a$  produced by the dipole at  $(0, y_a, h)$ . In our earlier

glide slope performance prediction report,\* it is shown that  $\vec{H}_a(\vec{r})$  is given by

$$\vec{H}_a(\vec{r}) = \frac{ikJ_0}{4\pi} \frac{e^{ikD_1}}{D_1^2} \left[ x\hat{e}_z - (z-h)\hat{e}_x \right] \quad (8)$$

where  $\hat{e}_x$ ,  $\hat{e}_y$ , and  $\hat{e}_z$  denote unit vectors in the x, y, and z directions respectively,  $J_0$  is a parameter which measures relative phase and amplitude, and  $D_1$  is the distance from the antenna to the observation point r:

$$D_1 = \left[ x^2 + (y-y_a)^2 + (z-h)^2 \right]^{1/2} \quad (9)$$

To take into account reflections from the ground plane ( $z = 0$ ) we use simple image theory to obtain the image field  $\vec{H}_a^*(\vec{r})$ :

$$\vec{H}_a^*(\vec{r}) = \frac{ikJ_0}{4\pi} \frac{e^{ikD_2}}{D_2^2} \left[ x\hat{e}_z - (z+h)\hat{e}_x \right] \quad (10)$$

where  $D_2$  is the distance from the image of the transmitting dipole to the field point  $\vec{r}$ :

$$D_2 = \left[ x^2 + (y-y_a)^2 + (z+h)^2 \right]^{1/2} \quad (11)$$

The total field intensity  $H_i$  at  $\vec{r}$  is just the sum of the direct ( $\vec{H}_a$ ) and ground reflected ( $\vec{H}_a^*$ ) signals:

$$\vec{H}_i(\vec{r}) = \vec{H}_a(\vec{r}) + \vec{H}_a^*(\vec{r}) \quad (12)$$

Note that on the ground plane ( $z = 0$ ), the z component of  $\vec{H}_i$  vanishes identically.

\* ILS Glide Slope Performance Predictions, Vol. B, FAA-RD-74-157.B, S. Morin, D. Newsom, D. Kahn, L. Jordan, September 1974.

The field  $H_i$  determined by Equations (8), (10), and (12) can now be substituted into Equation (7) and the integral can be performed over the illuminated surface of the scattering structure to give the scattered field at the receiver location  $r_1$ . Actually, only the  $z$  component of the scattered field need be calculated since the receiving antenna responds primarily to the horizontal component of electric field which is proportional to the  $z$  component of the magnetic field. It should be noted that for a complete solution, the contribution of the image of the scattering structure must also be calculated. We will assume that the receiver is always in the far field of the scattering structure so that the following asymptotic form of the gradient of the Green's function is applicable:

$$\vec{\nabla} G(\vec{r}_1, \vec{r}) \approx -ik (\vec{r}_1 - \vec{r}) \frac{e^{ik|\vec{r}_1 - \vec{r}|}}{|\vec{r}_1 - \vec{r}|^2} \quad (13)$$

Substituting Equations (8), (10), (12) and (13) into Equation (7) and taking the  $z$ -component of the resulting vector equation, we obtain the following expressions for  $H_{sz}(r_1)$ , the  $z$ -component of scattered magnetic field at the receiver point  $r_1$ :

$$H_{sz}(\vec{r}_1) = \frac{k^2 J_0}{8\pi^2} [I_1 + I_2 + I_3 + I_4] \quad (14)$$

where

$$I_1 = \int_{S_+} \frac{F_1}{D_1^2 R_1^2} e^{ik(R_1 + D_1)} ds \quad (15)$$

$$I_2 = - \int_{S_+} \frac{F_2}{D_2^2 R_1^2} e^{ik(R_1 + D_2)} ds \quad (16)$$

$$I_3 = \int_{S_+} \frac{F_1}{D_1^2 R_2^2} e^{ik(R_2 + D_1)} ds \quad (17)$$

$$I_4 = \int_{S_+} \frac{F_2}{D_2^2 R_2^2} e^{ik(R_2 + D_2)} ds \quad (18)$$

$$D_1 = [x^2 + (y - y_1)^2 + (z - h)^2]^{1/2} \quad (19)$$

$$D_2 = [x^2 + (y - y_1)^2 + (z + h)^2]^{1/2} \quad (20)$$

$$R_1 = [(X_1 - x)^2 + (Y_1 - y)^2 + (Z_1 - z)^2]^{1/2} \quad (21)$$

$$R_2 = [(X_1 - x)^2 + (Y_1 - y)^2 + (Z_1 + z)^2]^{1/2} \quad (22)$$

$$F_1 = n_1 \lambda (\bar{r}_1 - y) + [n_1 x + n_3 (z - h)] (X_1 - x), \quad (23)$$

$$F_2 = n_2 x (Y_1 - y) + [n_1 x + n_3 (z + h)] (X_1 - x) \quad (24)$$

In Equations (14) through (24), the coordinates  $(X_1, Y_1, Z_1)$  denote the coordinates of the aircraft.  $(x, y, z)$  the coordinates of some source point on the surface of the scattering structure and  $(n_1, n_2, n_3)$  the components of the unit outward normal to the surface of the scatterer at the point  $(x, y, z)$ . The integrals  $I_3$  and  $I_4$  represent the contributions of the image of the scattering structure in the ground plane  $z = 0$ . Note the following relationships among the four integrals:

$$\begin{aligned} I_1(X_1, Y_1, Z_1) &= -I_3(X_1, Y_1, -Z_1) \\ I_2(X_1, Y_1, Z_1) &= -I_4(X_1, Y_1, -Z_1) \end{aligned} \quad (25)$$

Consequently, when  $Z_1 = 0$ ,  $H_{sz}(\bar{r}_1) \equiv 0$  as it should be.

The direct numerical integration of the integrals  $I_1$ ,  $I_2$ ,  $I_3$ , and  $I_4$  for an arbitrary scattering structure would in general require an inordinate amount of computer time. However, certain simplifying assumptions can be made which considerably expedite the evaluation of these integrals. Specifically, we will assume that any scattering surface can be adequately represented by a series of interconnecting plane facets. By definition, the unit normal vector  $\hat{n}$  will be constant over each facet. The exact size, shape, and orientation of these facets will depend upon the surface characteristics of the particular scatterer. In turn, each facet can be broken up into a series of interconnected rectangular pieces. If these rectangular pieces are made small enough, the integrals  $I_1$ ,  $I_2$ ,  $I_3$  and  $I_4$  can be evaluated analytically for each piece and then the results summed over the whole surface of the scatterer to give  $H_{sz}$ . To illustrate these procedures, we will now evaluate the integral  $I_1$  for an arbitrarily oriented rectangular plate. In the course of this evaluation, we will discuss the size restrictions on such plates.

In Figure 2, a rectangular facet typical of those making up the surface of some scatterer has been drawn. We will evaluate the integral  $I_1$  of Equation (15) for such a facet in the Fraunhofer approximation. The unit vectors  $\hat{\eta}$  and  $\hat{\xi}$  lie in the plane of the facet, are orthonormal, and define the direction of the outward normal  $\hat{n}$ :

$$\hat{n} = \hat{\eta} \times \hat{\xi}$$

The center point of the facet  $(x_0, y_0, z_0)$  will be used as a local origin of coordinates for the integrations which are to be performed. The integral  $I_1$  is given by

$$I_1 = \int_{S_+} \frac{F_1}{D_1^2 R_1^2} e^{ik(D_1 + R_1)} ds \quad (26)$$

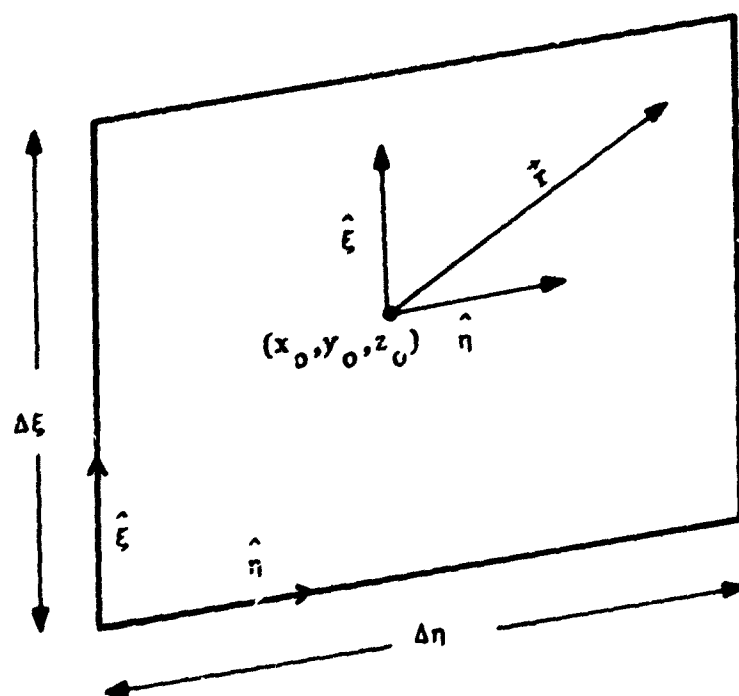


FIGURE 2. REPRESENTATION OF RECTANGULAR FACET

where

$$F_1 = n_2 x (Y_1 - y) + [n_1 x + n_3 (z - h)] (\bar{X}_1 - x) \quad (27)$$

$$D_1 = [x^2 + (y - y_a)^2 + (z - h)^2]^{1/2} \quad (28)$$

$$R_1 = [(X_1 - x)^2 + (Y_1 - y)^2 + (Z_1 - z)^2]^{1/2} \quad (29)$$

Clearly, the distances  $D_1$  and  $R_1$  denote, respectively, the length of the vector  $\vec{D}_1$  from the antenna to a point  $(x, y, z)$  on the surface of the facet and the length of the vector  $\vec{R}_1$  from the point  $(x, y, z)$  to the receiver. From Figure 2, it is seen that the vector  $\vec{D}_1$  can be represented as follows:

$$\vec{D}_1 = \vec{D}_{10} + \vec{r} \quad (30)$$

where

$$\vec{D}_{10} = x_0 \hat{e}_x + (y_0 - y_a) \hat{e}_y + (z_0 - h) \hat{e}_z \quad (31)$$

and

$$\vec{r} = \eta \hat{n} + \xi \hat{\xi} \quad (32)$$

and the ranges of the variables  $\eta$  and  $\xi$  are  $-\frac{\Delta\eta}{2} \leq \eta \leq \frac{\Delta\eta}{2}$  and  $-\frac{\Delta\xi}{2} \leq \xi \leq \frac{\Delta\xi}{2}$ . From Equation (30), we have

$$D_1 = D_{10} \left( 1 + \frac{r^2 + 2\vec{D}_{10} \cdot \vec{r}}{D_{10}^2} \right)^{1/2} \quad (33)$$

Normally,  $D_{10}$  is on the order of thousands of feet and  $r$  is of the order of tens of feet so that the radical in Equation (33) can be expanded in powers of  $r/D_{10}$  to give  $D_1$  approximately as a function of  $\eta$  and  $\xi$ . To terms of second order in  $r/D_{10}$ , we obtain

$$D_1 \approx D_{10} + \eta \cos \alpha + \xi \cos \beta + \frac{r^2}{2D_{10}} + \frac{(\vec{D}_{10} \cdot \vec{r})}{D_{10}^2} \quad (34)$$



where

$$\hat{D}_{10} = \vec{D}_{10}/D_{10} \quad (35)$$

$$\cos \alpha = \hat{D}_{10} \cdot \hat{\eta} \quad (36)$$

$$\cos \beta = \hat{D}_{10} \cdot \hat{\xi} \quad (37)$$

The numbers  $\cos \alpha$  and  $\cos \beta$  are the direction cosines of  $D_{10}$  relative to  $\hat{\eta}$  and  $\hat{\xi}$ . In the Fraunhofer approximation which we will use, it is assumed that the quadratic terms of Equation (33) are small compared to a wavelength for any point  $(x, y, z)$  on the surface of the facet so that we can write to a good approximation:

$$D_1 = D_{10} + \eta \cos \alpha + \xi \cos \beta \quad (38)$$

It can be shown that the largest value attainable by the quadratic terms in Equation (33) on the facet's surface is

$$\Delta = \frac{(\Delta \eta)^2}{8 D_{10}} \sin^2 \alpha + \frac{(D \xi)^2}{8 D_{10}} \sin^2 \beta + \frac{\Delta \eta \Delta \xi}{4} |\cos \alpha \cos \beta| \quad (39)$$

Equation (38) should provide a good approximation for the distance  $D_1$  as a function of  $\eta$  and  $\xi$  as long as  $\Delta \eta$  and  $\Delta \xi$  are chosen so that  $\Delta$  in Equation (39) is small compared to the wavelength  $\lambda$ . We will return to this important requirement later.

Similarly, the vector  $\vec{R}_1$  can be represented as follows:

$$\vec{R}_1 = \vec{R}_{10} - \vec{r} \quad (40)$$

$$\text{where } \vec{R}_{10} = (X_1 - x_0)\hat{e}_x + (Y_1 - y_0)\hat{e}_y + (Z_1 - z_0)\hat{e}_z \quad (41)$$

Thus, in the Fraunhofer approximation, we find

$$R_1 = R_{10} - \eta \cos \alpha - \xi \cos \beta \quad (42)$$

$$\cos \alpha = \frac{\hat{R}_{10}}{R_{10}} \hat{\eta} \quad (43)$$

$$\cos \delta = \frac{\hat{R}_{10}}{R_{10}} \hat{\xi} \quad (44)$$

$$\text{where } \hat{R}_{10} = \vec{R}_{10}/R_{10} \quad (45)$$

In Equation (42), we have ignored terms of second order and higher in  $r/R_{10}$ .

One final approximation which we will make is that  $\Delta\eta$  and  $\Delta\xi$  are sufficiently small compared with  $D_{10}$  and  $R_{10}$ , that the variation of the amplitude function  $F_1/D_1^2 R_1^2$  in Equation (26) can be ignored. This is normally an excellent approximation. Consequently, we will assume that for any point on the surface of the facet we can write

$$F_1/D_1^2 R_1^2 = F_{10}/D_{10}^2 R_{10}^2 \quad (46)$$

where  $F_{10}$ ,  $D_{10}$ , and  $R_{10}$ , are the values of  $F_1$ ,  $D_1$ , and  $R_1$  at the center point  $(x_0, y_0, z_0)$ .

Substituting Equations (38), (42), and (46) into Equation (26) yields the following approximate expression for  $I_1$ :

$$I_1 = \frac{F_{10}}{D_{10}^2 R_{10}^2} e^{ik(D_{10}+R_{10})} \int_{-\Delta\eta/2}^{+\Delta\eta/2} e^{ik\eta(\cos\alpha - \cos\gamma)} d\eta \int_{-\Delta\xi/2}^{+\Delta\xi/2} e^{ik\xi(\cos\beta - \cos\delta)} d\xi \quad (47)$$

Performing the integrals indicated in Equation (47), we finally obtain the following approximate expression for  $I_1$ :

$$I_1 = \frac{4F_{10}}{D_{10}^2 R_{10}^2} \frac{e^{ik(D_{10}+R_{10})}}{k^2} \times \frac{\sin\left\{\frac{k\Delta\eta}{2}(\cos\alpha - \cos\gamma)\right\}}{(\cos\alpha - \cos\gamma)} \frac{\sin\left\{\frac{k\Delta\xi}{2}(\cos\beta - \cos\delta)\right\}}{(\cos\beta - \cos\delta)} \quad (48)$$

A similar treatment of the integrals  $I_2$ ,  $I_3$ , and  $I_4$  ultimately lead to the following approximate expression for the scattered magnetic field intensity at the receiver due to the rectangular facet:

$$\begin{aligned}
 H_{sz}(\vec{r}_1) = & \frac{J_0}{2\pi^2} \frac{F_{10} e^{ik(D_{10}+R_{10})}}{D_{10}^2 R_{10}^2} \frac{\sin(kA\Delta\eta/2)\sin(kB\Delta\xi/2)}{AB} \\
 & - \frac{J_0}{2\pi^2} \frac{F_{20} e^{ik(D_{20}+R_{10})}}{D_{20}^2 R_{10}^2} \frac{\sin(kA_1\Delta\eta/2)\sin(kB_1\Delta\xi/2)}{A_1 B_1} \\
 & - \frac{J_0}{2\pi^2} \frac{F_{10} e^{ik(D_{10}+R_{20})}}{D_{10}^2 R_{20}^2} \frac{\sin(kA_2\Delta\eta/2)\sin(kB_2\Delta\xi/2)}{A_2 B_2} \\
 & + \frac{J_0}{2\pi^2} \frac{F_{20} e^{ik(D_{20}+R_{20})}}{D_{20}^2 R_{20}^2} \frac{\sin(kA_3\Delta\eta/2)\sin(kB_3\Delta\xi/2)}{A_3 B_3} \quad (49)
 \end{aligned}$$

where  $F_{10}$ ,  $F_{20}$ ,  $D_{10}$ ,  $D_{20}$ ,  $R_{10}$  and  $R_{20}$  denote the values of  $F_1$ ,  $F_2$ ,  $D_1$ ,  $D_2$ ,  $R_1$ , and  $R_2$  at  $(x_0, y_0, z_0)$  and the parameters  $A$ ,  $A_1$ ,  $A_2$ ,  $A_3$ ,  $B$ ,  $B_1$ ,  $B_2$ , and  $B_3$  are defined as follows:

$$A = \cos\alpha - \cos\gamma \quad B = \cos\beta - \cos\delta \quad (50)$$

$$A_1 = \cos\alpha_1 - \cos\gamma \quad B_1 = \cos\beta_1 - \cos\delta \quad (51)$$

$$A_2 = \cos\alpha - \cos\gamma_1 \quad B_2 = \cos\beta - \cos\delta_1 \quad (52)$$

$$A_3 = \cos\alpha_1 - \cos\gamma_1 \quad B_3 = \cos\beta_1 - \cos\delta_1 \quad (53)$$

and the angles appearing in Equations (50) through (53) are defined as follows:

$$\vec{D}_{10} = x_0 \hat{e}_x + (y_0 - y_a) \hat{e}_y + (z_0 - h) \hat{e}_z \quad (54)$$

$$\vec{R}_{10} = (x_1 - x_0) \hat{e}_x + (y_1 - y_0) \hat{e}_y + (z_1 - z_0) \hat{e}_z \quad (55)$$

$$\vec{D}_{20} = x_0 \hat{e}_x + (y_0 - y_a) \hat{e}_y + (z_0 + h) \hat{e}_z \quad (56)$$

$$\vec{R}_{20} = (x_1 - x_0) \hat{e}_x + (y_1 - y_0) \hat{e}_y - (z_1 + z_0) \hat{e}_z \quad (57)$$

and

$$\cos \alpha = \frac{\vec{D}_{10} \cdot \hat{\eta}}{D_{10}}, \quad \cos \beta = \frac{\vec{D}_{10} \cdot \hat{\xi}}{D_{10}} \quad (58)$$

$$\cos \alpha_1 = \frac{\vec{D}_{20} \cdot \hat{\eta}}{D_{20}}, \quad \cos \beta_1 = \frac{\vec{D}_{20} \cdot \hat{\xi}}{D_{20}} \quad (59)$$

$$\cos \alpha = \frac{\vec{R}_{10} \cdot \hat{\eta}}{R_{10}}, \quad \cos \beta = \frac{\vec{R}_{10} \cdot \hat{\xi}}{R_{10}} \quad (60)$$

$$\text{and } \cos \alpha_1 = \frac{\vec{R}_{20} \cdot \hat{\eta}}{R_{20}}, \quad \cos \beta_1 = \frac{\vec{R}_{20} \cdot \hat{\xi}}{R_{20}} \quad (61)$$

The total scattered field at the receiver is obtained by summing up the contributions from all of the rectangular facets which make up the surface of the scattering structure. Segmenting the surface of a scatterer into rectangular facets and then applying the approximate closed form solution in Equation (49) to each facet represents a far more efficient procedure for calculating the scattered field at the receiver than attempting to directly numerically integrate Equations (14) through (18).

We now return to the question raised earlier of the size restrictions upon the facets. Clearly, one would like to maximize the area of each facet in order to minimize computer running time. The principal restriction upon the size of the facets is that  $\Delta\eta$  and  $\Delta\xi$  must not be so large that the Fraunhofer approximation, upon which the approximate formula (49) is based, is violated. That is, the quadratic path length difference terms like those in Equation (34)

must be small compared to the wavelength  $\lambda$  for all points on the surface of the facet to which Equation (49) is to be applied. Thus, in choosing appropriate values for  $\Delta\eta$  and  $\Delta\xi$ , we are essentially faced with an optimization problem with a constraint. Specifically, we want to maximize the area  $\Delta\eta\Delta\xi$  of the facet while keeping the quadratic path length difference terms less than some prescribed value. For example, for the path length  $D_1$ , the maximum value of the quadratic path length difference term is given by

$$\Delta = \frac{(\Delta\eta)^2}{8 D_{10}} \sin^2 \alpha + \frac{(\Delta\xi)^2}{8 D_{10}} + \frac{\Delta\eta\Delta\xi}{4} |\cos\alpha\cos\beta| \quad (62)$$

Depending upon the sign of  $\cos\alpha\cos\beta$ , this value will be achieved at two of the four corners of the rectangular facet. At all other points, the quadratic path length terms will be less than  $\Delta$ , but always positive. We can optimize our choice of  $\Delta\eta$  and  $\Delta\xi$  by maximizing  $\Delta\eta\Delta\xi$  subject to the condition that  $\Delta$  in Equation (62) be some fractional part of a wavelength. This problem has been solved in closed form using Lagrange multipliers. The optimization procedure must be applied to the quadratic path length difference terms affecting all four distances ( $D_1$ ,  $D_2$ ,  $R_1$ ,  $R_2$ ) and then from the resulting set of solutions the smallest values of  $\Delta\eta$  and  $\Delta\xi$  are chosen. A subroutine has been written to carry out the optimization procedure.

Of course, the scattered fields must be calculated for each dipole in the array, the parameter  $J_0$  being varied to take into account the exact phase and amplitude ratios among the various elements and, along with  $J_0$ , the height  $h$  and y-offset  $y_a$  of each element. Our program automatically offsets the elements of an array to correct for the effects of proximity phase lag. The y-coordinates of the elements are adjusted so that all dipoles are at the same slant distance from the touchdown point on the runway directly opposite the array.

Once all of the scattered fields have been calculated, the calculation of the difference in depth of modulation (D.D.M) at a given receiver location is straight forward. The scattered fields at the carrier frequency, 90Hz modulated frequency, and 150Hz modulated frequency are first added to the direct fields at those frequencies. By direct fields is meant the fields which would exist if the scatterers were not present. For example, if the ground plane is perfectly flat, the direct field for any one of the three frequencies at the receiver location  $r_1$  is just the z component of Equation (12).

$$H_{1z}(\vec{r}_1) = \frac{ikJ_0}{4\pi} x_1 \left[ \frac{e^{ikD_1}}{D_1^2} - \frac{e^{ikD_2}}{D_2^2} \right] \quad (63)$$

where, here,  $D_1$  and  $D_2$  denote, respectively, the distance from the antenna to the aircraft and the distance from the image antenna to the aircraft, and  $x_1$  is the x coordinate of the aircraft. If the ground plane is not perfectly flat or at least nearly so the direct fields are calculated differently. These alternate procedures will be discussed in the next section. In any case, once the total complex field amplitudes (direct plus scattered summed for all dipoles in the array) have been found, the DDM is calculated as follows: let  $H_c$ ,  $H_{150}$ , and  $H_{90}$  denote the total complex amplitudes at the carrier frequency, the 150 Hz modulated frequency, and the 90 Hz modulated frequency. In terms of these complex amplitudes, the difference in depth of modulation is given by:

$$D.D.M. = \text{Re} \left( \frac{H_{150} - H_{90}}{H_c} \right) \quad (64)$$

where Re denotes the real part of the complex number. Full scale deflection (150 microamps) corresponds to a D.D.M. of .175 for the glide slope. Consequently, the C.D.I. (course deviation indication) is given by

$$C.D.I. = 857.14 \text{ Re} \left( \frac{H_{150} - H_{90}}{H_c} \right) \text{ microamps} \quad (65)$$

## PART B

In Part A of this section, we developed techniques for estimating glide slope performance degradation due to multipath scattering. Once the scattered fields produced by the various scattering structures in the airport environment have been calculated, they are added to the direct fields at the corresponding frequencies and from these total fields, the C.D.I. is calculated using Equation (62). The direct field at the particular frequency is just the field which would be detected at the receiver in the absence of the scattering structures. If the ground plane is otherwise perfectly flat or nearly so, the direct field is given according to simple image theory by Equation (63).

$$H_{iz} = \frac{ikJ_0}{4\pi} X_1 \left[ \frac{e^{ikD_1}}{D_1^2} - \frac{e^{ikD_2}}{D_2^2} \right] \quad (63)$$

where  $D_1$  and  $D_2$  are, respectively, the distance between the receiver and the transmitting dipole and between the receiver and the image of the dipole. On the other hand, if the terrain profile exhibits significant irregularities such as downgrade; or drop offs along the line of sight between the aircraft and the antenna mast, Equation (63) cannot be used and the techniques developed in our earlier glide slope performance prediction model must be used.

In the report ILS Glide Slope Performance Prediction, Vol. B (FAA-RD-74-157.B), we developed mathematical procedures for calculating the ground reflected signals resulting from irregular terrain profiles such as the one depicted in Figure 3. The detailed calculations will not be repeated here, However, the updated computer program contains the subroutines for performing these calculations. One simply inputs the shape of the terrain profile along the line of sight between the aircraft and the antenna mast, and the subroutines

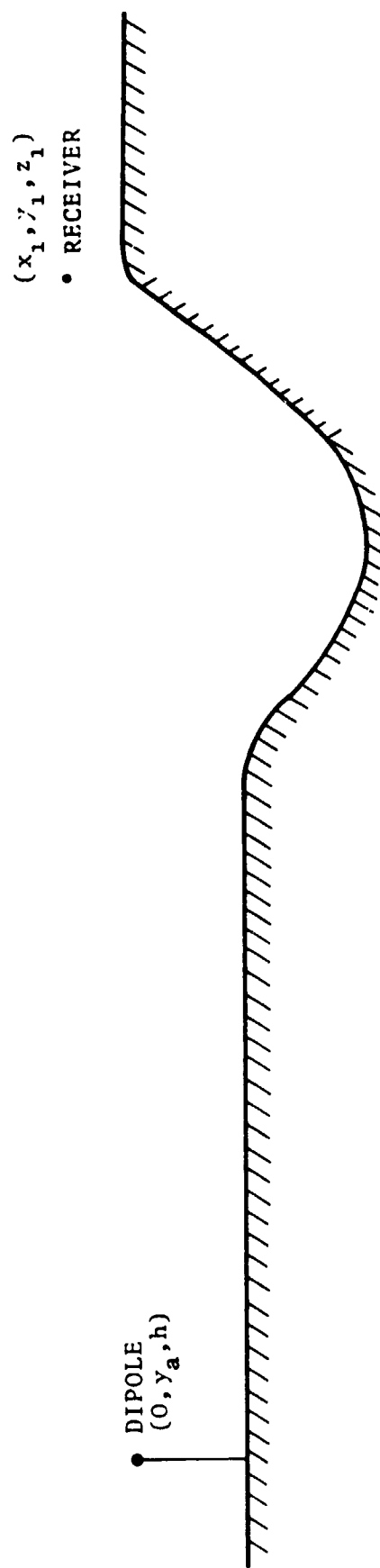


FIGURE 3. TYPICAL PROFILE OF ONE-DIMENSIONAL TERRAIN VARIATION



will generate the ground reflected signals at the carrier frequency, 90Hz modulated frequency, and the 150Hz modulated frequency. These signals are then combined with the incident signals directly from the antennas to give what we have been calling the direct fields, the fields which would be measured at the receiver assuming that no scatterers (hangars, hillsides, etc.) were present. These direct signals are then combined with the scattered signals calculated using the techniques of Part A and the resulting total signals are used in Equation (65) to calculate C.D.I. Again, if the terrain profile is perfectly flat or nearly so, Equation (63) can be used to calculate the direct signals.

### 3. NUMERICAL RESULTS

Before presenting some sample numerical results illustrating the predictions of our model, we will first review the characteristics of the three main types of image glide slope arrays; the null reference, the sideband reference, and the capture effect arrays.

The null reference array is the simplest of the image glide slope systems. It consists of two transmitting antennas whose heights are in the ratio of 2:1. The upper antenna is fed sideband only signal, the 150 Hz and the 90 Hz components being of equal amplitude but 180° out of phase. The lower antenna is fed both carrier and sideband. The carrier signal is nominally 40% modulated. The ratio of the sideband currents in the upper antenna to the sideband currents in the lower antenna is typically 0.3. The sideband ratio of 0.3 would nominally yield a 1.4° course width (full deflection 0.7° above or below the glide path). Let

$I_c$ ,  $I_{150}$ , and  $I_{90}$  denote the current amplitudes fed to the antennas at the carrier frequency, the 150 Hz modulated frequency, and the 90 Hz modulated frequency, respectively. The null reference array parameters discussed above can be summarized as follows:

<u>Carrier Antenna</u>	<u>Sideband Antenna</u>
Height = $h$	Height = $2h$
$I_c = 1$	$I_c = 0$
$I_{150} = 0.4$	$I_{150} = 0.12$
$I_{90} = 0.4$	$I_{90} = -0.12$

Note that all current amplitudes have been normalized relative to the carrier current amplitude ( $I_c = 1$ ).

The sideband reference array employs two transmitting dipoles whose heights are in the ratio of 3:1. If the lower antenna is positioned at 1/2 the height of the lower antenna of the null reference array and if the upper antenna is positioned at 3/4 of the height of the upper antenna of the null reference array, the same glide angle is produced. Modulated carrier (40% modulated) is fed to the lower antenna. Both antennas are fed separate sideband signals. The separate sideband signals fed to the two antennas are equal in amplitude but are 180° out of phase. The amplitude ratio of the separate sideband signal to the carrier sideband signal is typically 0.3. This ratio produces a nominal course width of 1.4° as in the case of the null reference array. The sideband reference parameters are summarized below.

<u>Lower Antenna</u>	<u>Upper Antenna</u>
Height = $h$	Height = $3h$
$I_c = 1$	$I_c = 0$
$I_{150} = 0.28$	$I_{150} = 0.12$
$I_{90} = 0.52$	$I_{90} = -0.12$

Note that the  $I_{150}$  and  $I_{90}$  current amplitudes given above for the lower antenna represent the sums of the carrier sideband and separate sideband signals ( $I_{150} = .4 - .12 = .28$ ,  $I_{90} = .4 + .12 = .52$ ). All current amplitudes have been normalized relative to the carrier signal amplitude.

The capture effect glide slope array consists of three transmitting antennas whose heights are in the ratios of 1:2:3. If the lower and middle antennas are set at the same heights as the null reference antennas, the same glide angle is produced. We will not treat the clearance signal which provides a ~~slight~~ fly up signal at low approach angles but has little effect upon the glide angle and course width. Concerning the primary signal, the modulated carrier is fed to both the lower and middle antennas. The modulated carrier fed to the middle antenna has half the amplitude and is  $180^\circ$  out of phase with the modulated carrier fed to the lower antenna. The carrier signals are nominally 40% modulated. In addition, all three antennas are fed separate sideband signals. The separate sideband signals fed to the lower and upper antennas have half the amplitude and are  $180^\circ$  out of phase with the separate sideband signal fed to the middle antenna. The ratio of the separate sideband signal fed to the middle antenna to the carrier sideband signal in the lower antenna is typically 0.3. This ratio yields nominally a course width of  $1.4^\circ$  as in the case of the null reference array. The capture effect array parameters are summarized below.

Lower Antenna

Height = h

$I_c = 1$

$I_{150} = 0.34$

$I_{90} = 0.46$

Middle Antenna

Height = 2h

$I_c = -0.5$

$I_{150} = -0.08$

$I_{90} = -0.32$

Upper Antenna

Height = 3h

$I_c = 0$

$I_{150} = -0.06$

$I_{90} = 0.06$

Note that the  $I_{150}$  and  $I_{90}$  current amplitudes given above represent the sums of the carrier sideband and separate sideband signals. Again, all values have been normalized relative to the carrier amplitude in the lower antenna.

It should be noted here that our computer program automatically offsets the elements of each glide slope array to correct for the effects of proximity phase lag. The y coordinates of the elements are adjusted so that all dipoles are at the same slant distance from the touchdown point on the runway directly opposite the array. For each array, one element is held fixed while the other elements are offset relative to the fixed one. For the null reference and sideband reference arrays, the lower element is held fixed while for the capture array, the middle element is held fixed. The amount of the offset for each dipole can be calculated approximately in the following manner. Let  $y_a$  and  $h$  denote, respectively, the y-coordinate and height of the fixed antenna element. The y-displacement,  $\epsilon$ , of any other element in the array relative to the fixed one is given approximately by:

$$\epsilon = \frac{h^2 - H^2}{2y_a} \quad (66)$$

where  $H$  is the height of the element which is to be offset.

For the present study, the wavelength  $\lambda$  was set at 3 feet. All arrays were positioned 300 feet from the centerline of the runway. The heights of the array elements were set at 14.33 feet and 28.66 feet (approximately  $5\lambda$  and  $10\lambda$ ) for the null reference array, 7.17 feet and 21.5 feet (approximately  $2.5\lambda$  and  $7.5\lambda$ ) for the sideband reference array, and 14.33 feet, 28.66 feet, and 42.99 feet (approximately  $5\lambda$ ,  $10\lambda$ , and  $15\lambda$ ) for the capture effect array. Under normal circumstances, a glide angle of  $3^\circ$  would be produced by all three arrays.

To illustrate the performance of our multipath model, the glide slope course deragation caused by a large, flat reflecting surface (perhaps the side of a large hangar or the side of a hill) has been calculated. The structure was taken to be 300 feet long and 100 feet high and was oriented parallel to the runway centerline. The structure was positioned 200 feet from the runway centerline in the y-direction, on the opposite side of the centerline from the glide slope array. The near edge of the structure was displaced 1000 feet in the x-direction from the touchdown point. The geometry of the configuration is depicted in Figure 4.

In Figures 5, 6, and 7 are plotted the C.D.I. signal as a function of the horizontal distance from touchdown for each of the three arrays for the arrangement depicted in Figure 4. In each case, the receiver followed the nominal  $3^\circ$  zero C.D.I. hyperbola. The results for all three arrays are very similar. Our model predicts large high frequency, alternating fly up and fly down signals near the end of the flight path roughly between 1700 feet and 1800 feet from touchdown. This region in fact corresponds almost exactly to the region of specular reflection as predicted by geometrical optics. Note that the excursions are large enough to saturate the receiver over much of the affected range (full scale deflection = 150 microamps). The excursions are clearly highly localized and damp out very rapidly as the aircraft leaves the specular reflection zone. The narrowness of the pattern (i.e., the lack of broadening due to diffraction and the rapid damping of the side lobes) is undoubtedly attributable to the large size of the scatterer relative to the scattering wavelength.

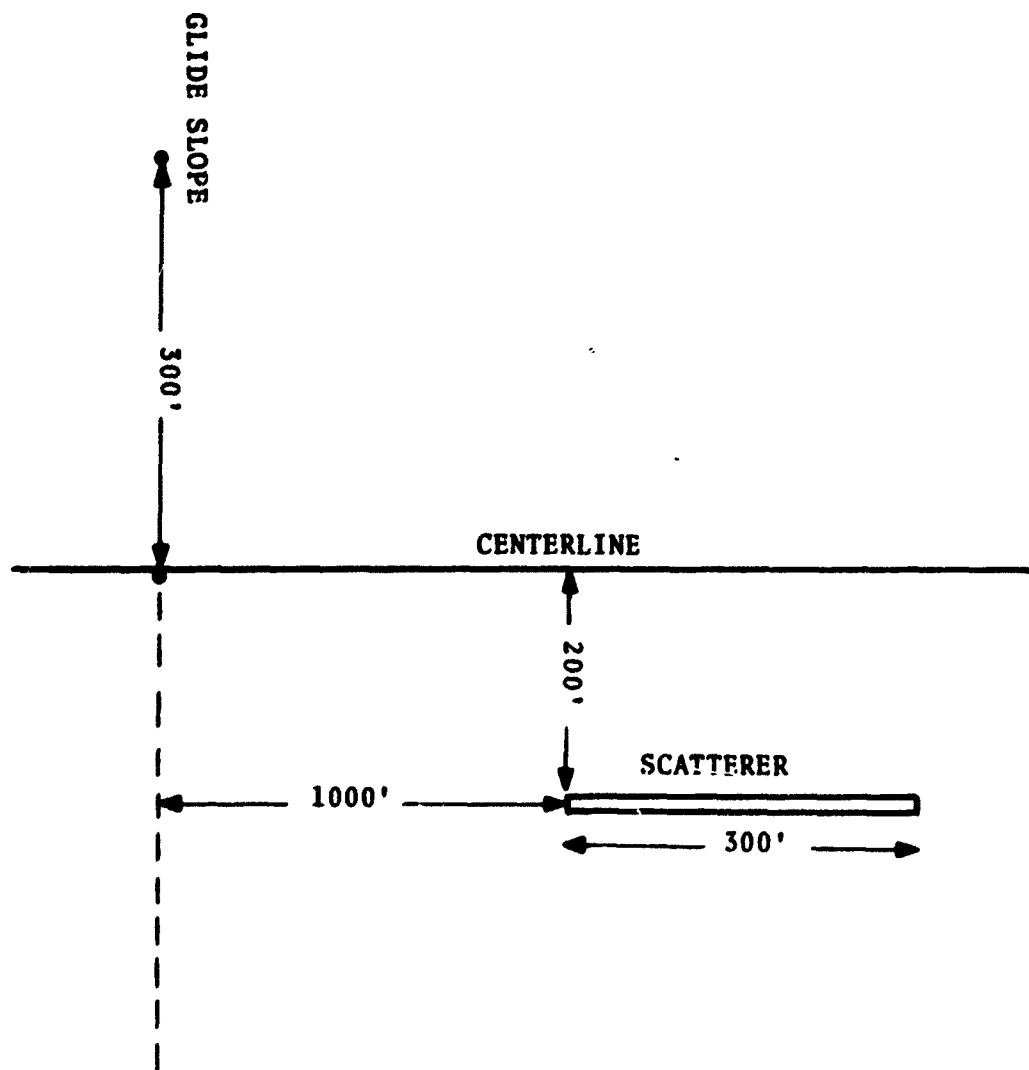


FIGURE 4. OVERVIEW OF A MULTIPATH CONFIGURATION

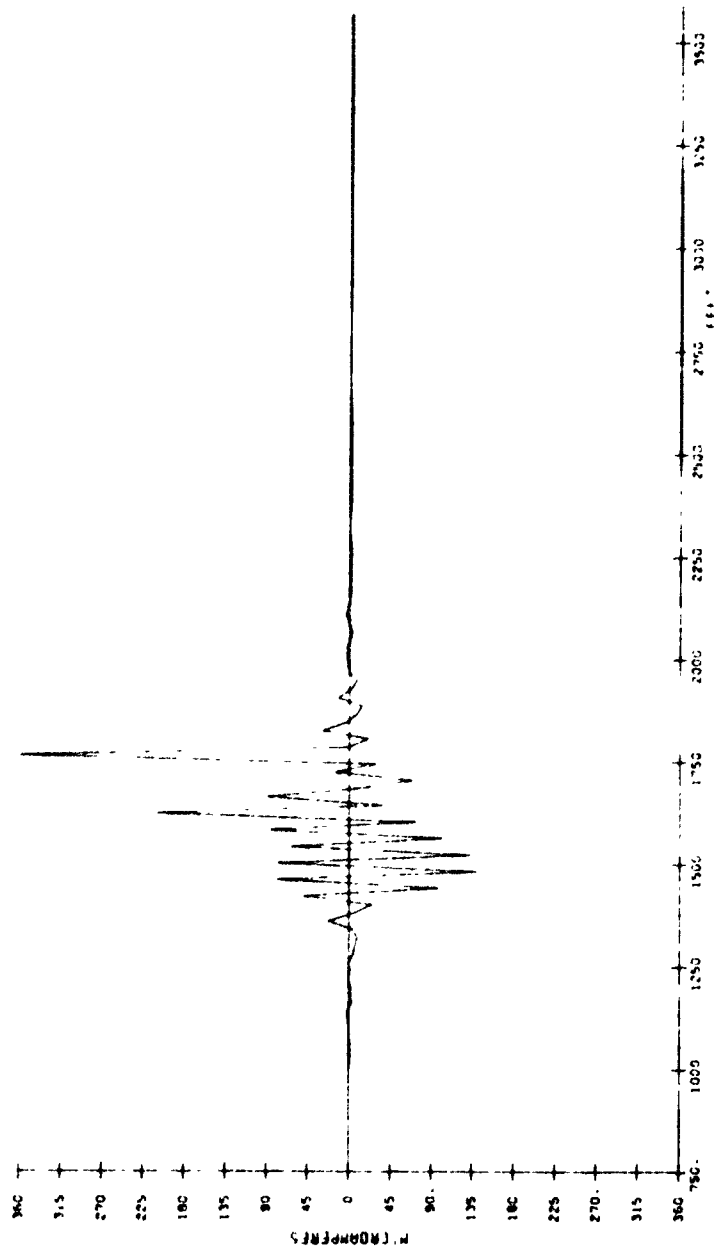


FIGURE 5. NULL REFERENCE ARRAY, FLYABILITY RUN

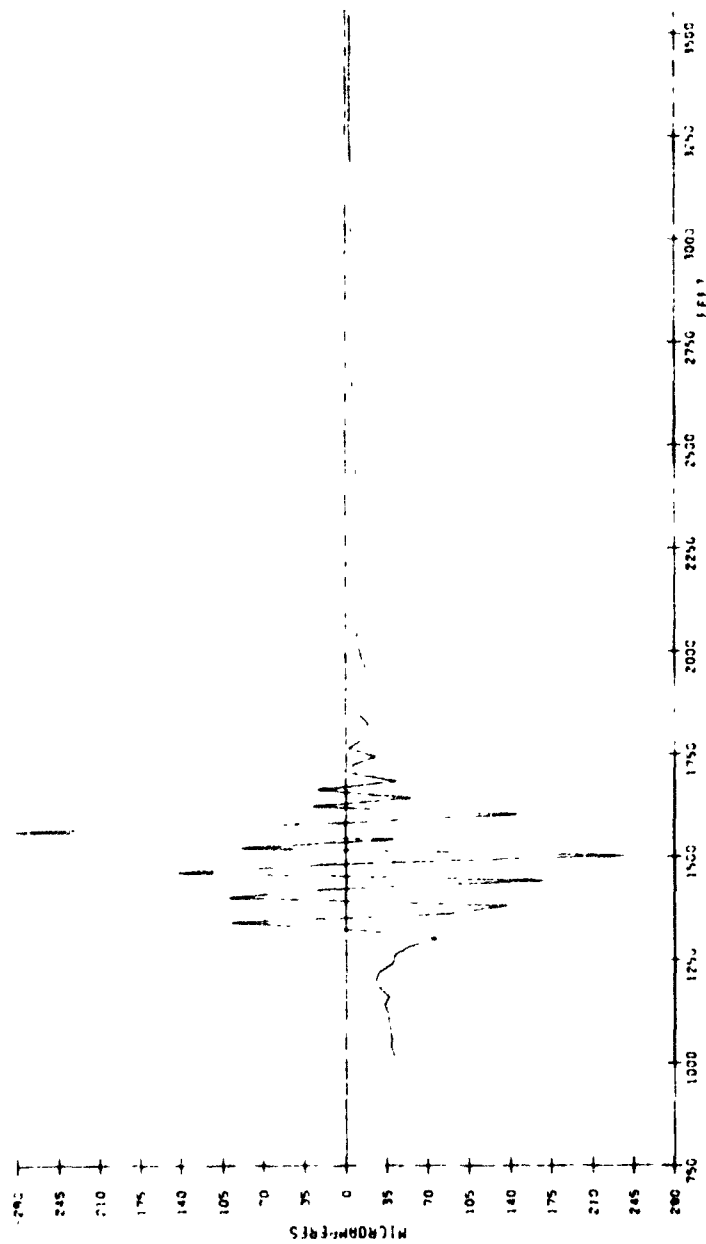


FIGURE 6. SIDEBAND REFERENCE ARRAY, FLYABILITY RUN



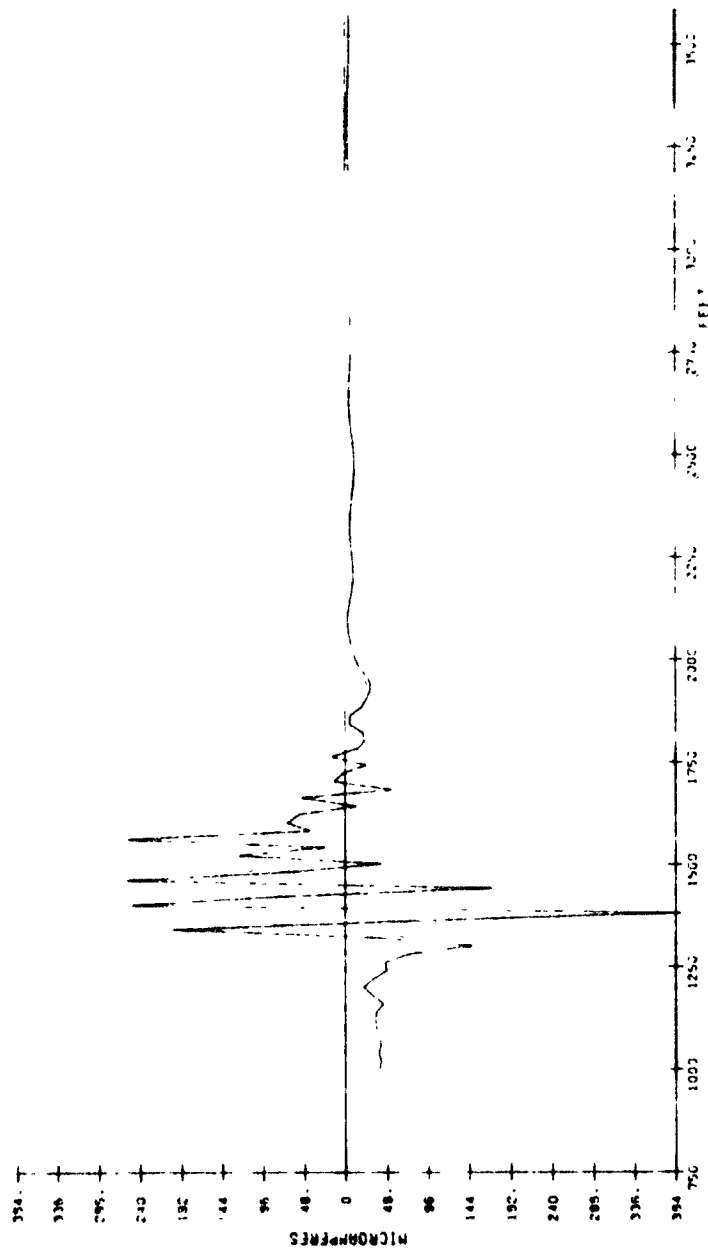


FIGURE 7. CAPTURE EFFECT ARRAY, FLYABILITY RUN

# PROGRAM ILSVEN.F4

```

1  DIMENSION ILABL(8)
2  DIMENSION IPTVAL(33)
3  COMMON /PLOT/ XPR,RYN,NHMX,REFI,RELT,RYTH,NHIX,NYI,PLY,T,
4  IPRN,NHIX,REFI,RELT,RYTH,NHIX,REFI,RELT,
5  ZAXN,NHIX,REFI,RELT,RYTH,NHIX,REFI,RELT,
6  RADIN,ADIA,ADIE,ADIL,
7  RADIN,ADIA,ADIE,ADIL,
8  RADIN,ADIA,ADIE,ADIL,
9  EQUIVALENCE (IPTVAL(1),NRP)
10  IMPLICIT COMPLEX (C)
11  DIMENSION X(20),Y(20),Z(20)
12  DIMENSION CF1(20),CF2(20),CF3(20)
13  IMPLICIT DOUBLE PRECISION (D)
14  COMMON /REC/RY,RY,RY,RZ,RT,RSIZE
15  REAL LAMBDA
16  COMMON /GROUND/ R,X1(20),Z1(20),X2(0/20),Z2(0/20),ZL
17  COMMON /VAL/ NR,NI
18  C THIS VALUE OF TWO PI IS INITIALIZED THIS WAY TO AVOID USING
19  C BLACK DATA
20  DPI=6.2831853071795864769
21  C THIS OPENS THE OUTPUT FILE
22  CALL OFILELL,"STRIP")
23  C THIS SUBROUTINE OPENS THE FLIGHT PATH FILE AND RETURNS WITH
24  C THE FLIGHT PATH PLOT LABEL (ILABL) AND TIME CONSTANT (TAU)
25  C THE FILE WAS SET UP WITH JOVNAH SO THIS SUBROUTINE AND INPUT ARE
26  C USED TO FACILITATE MODIFICATIONS
27  CALL IFILABEL,TAU)
28  WRITE(1,1000) ILABL,TAU
29  C THIS SECTION INITIALIZES SOME CONSTANTS
30  WRPEO
31  C THIS SECTION INPUTS THE GROUND STRIP DESCRIPTIONS
32  CALL IFILE(20,"GRND")
33  READ(20,1000) ILABL
34  WRITE(1,1000) ILABL
35  READ(20) R,X1,Z1,X2,Z2
36  CALL RELEASES (20)
37  C THIS SECTION INPUTS THE ANTENNA FILE NAME TO BE USED.
38  C AND THEN INPUTS THE ANTENNA ELEMENT DESCRIPTIONS
39  WRITE(1,2001)
40  FORMAT(' INPUT ANTENNA FILE NAME: ',8)
41  READ(1,2001) ILABL
42  CALL IFILE(20,ILABL)
43  READ(20,1000) ILABL
44  WRITE(1,1000) ILABL
45  READ(20) LAMBDA,NEL,X(1),Y(1),Z(1),CF1(1),CF2(1),CF3(1),IS1,NEL)

```

```

54  WRITE(1) LAMBDA,DEL, (X(1),Y(1),Z(1),CP1(1),CP2(1),CP3(1),CP4(1),CP5(1))
55  CALL HELPAS (20)
56  SORTLST1=1/SORT(2,0,LAMBDA)
57  Y=1/2*LAMBDA
58  DAREMPI/DREL(LAMBDA)
59  DAREMGI(DAY)
60
61  THIS IS THE MAIN LOOP FOR THE SIMULATION, THE RECEIVING
62  LOCATION IS READ IN BY INPUT, THE DATA IS : 1000000000
63  C THE INPUT BEING DONE BY JMWAPX, IF THERE ARE 3 WIRE RECEIVERS
64  C POINTS THE SUBROUTINE RETURNS TO 200.
65  201 CALL INPUT(200)
66
67  THIS SECTION INITIALIZES THE COMPLEXA AND ITURNS FOR
68  C THE RECEIVED FIELD AS FOLLOWS:
69  C
70  C CP1 CAPWIRE WITH "IDEAL" GROUND
71  C CP2 150 M2 STRIPWIRE WITH "IDEAL" GROUND
72  C CP3 90M2 STRIPWIRE WITH "IDEAL" GROUND
73  C CP4 CAPWIRE WITH "IDEAL" FLAT GROUND PLANE
74  C CP5 150M2 WITH "IDEAL" GROUND
75  C CP6 90 M2 WITH "IDEAL" GROUND
76  C CP7(0,0,0)
77  C CP8(0,0,0)
78  C CP9(0,0,0)
79  C CP10(0,0,0)
80  C CP11(0,0,0)
81  C CP12(0,0,0)
82  W2SORT(RX00R0202)
83
84  THIS LOOP IS OVER THE ELEMENTS OF THE ANTENNA
85  C THE COMPLEX FIELDS ARE SUMMED IN CP1,CP2 ETC.
86  DO 3 IFLST,REL
87
88  THESE ARE THE LOCATION COORDINATES OF THE ANTENNA ELEMENTS
89  C AND CONSTANTS USED IN THE STRIP INTEGRATION
90  AX0X(1EL)
91  AY0Y(1EL)
92  AZ0Z(1EL)
93  DELX0X-AZ
94  DELY0Y-AZ
95  DELZ0Z-AZ
96  W2SORT(DELX0DELX+DELY0DELY+DELZ0DELZ)
97  W2SNGL(DP)
98  DAREMPI/DPI
99
100  THIS SECTION INITIALIZES NM AND HT TO INCLUDE THE
101  C SEMI-INFINITE PEAK GROUND PLANE
102  TEMP2=DR-NBLK(FLNAT(1L))001
103  TEMP02=AZ
104  F1=1/SORT(TEMP02*AT0AY)
105  F2=1/SORT(TEMP02*AT0F1)
106  F3=1/SORT(1.0*AT0AY/(TEMP02*TEMP02))

```

```

107      THERCOAS
108      R12M20TC
109      SUBST((1./M2+1./M2)/(TCOTCOTC))
110      GEAR/(THERCOAS)
111      TEMPASAREF1
112      SFMS1*(TFM)
113      PCOS(TFMP)
114      TEMPAS2G/DAR/H2
115
116      M AND M1 ARE THE REAL & IMAGINARY PARTS OF THE COMPLEX
117      *GAIN* FACTOR OF THE GROUND SURFACE SCATTERING IN THE MICROWAVE
118      C LOCATION
119      MMS-TEMP*(SF/PC/(DARETD))
120      M1=TEMP*(PC-SF/(DARETD))
121
122      C THIS SUBROUTINE SUMS THE *GAIN* FACTOR FOR EACH STATION IF
123      C THE GROUND SURFACE
124      CALL SCAT
125
126      C THIS SECTION INCLUDES THE EFFECT OF THE DIRECT RADIATION FROM
127      C THE ANTENNA ELEMENT AT THE RECEIVER
128      MMS=TEMP12L
129      M1=TEMP12L
130      TEMPDELE/(MMS)
131      SF=SF1*(TFM2)
132      PC=PC1*(TFM2)
133
134      C TEMP IS THE COMPLEX GAIN FACTOR INCLUDING ALL RADIATION FROM
135      C THIS ELEMENT
136      CTEMP=CMPLX(-TEMP*SF+MMS*M1,TEMP*(C+MMS*M1)).5/LA-DBA
137
138      C THIS SECTION ACCUMULATES THE VALUES IN THE VARIOUS FREQUENCY CIES
139      CFS1=CF21+CTEMP*CF1(IE1)
140      CFS2=CF22+CTEMP*CF2(IE1)
141      CFS3=CF23+CTEMP*CF3(IE1)
142      ALPHASARE2=.5/AMRDA*CMPLX(-SF,PC)
143      CTEMP=TEMP*.5/AMRDA*CMPLX(-SF,PC)
144      ICPLX((1.-COS(ALPH1))-SIN(ALPH1))
145      CFS1=CF1+CTEMP*CF1(IE1)
146      CFS2=CF2+CTEMP*CF2(IE1)
147      CFS3=CF3+CTEMP*CF3(IE1)
148
149      3      CONTINUE
150      WRITE(1,200) M1,M2,P1,CFM1,CFM2,CFM3,CFM1,CFM2,CFM3
151      FORMAT(4F,7E13.6,/,0E13.6)
152      GO TO 201
153
154      C THIS IS THE TERMINATION SECTION. THE INITIAL RECORD ON
155      C THE OUTPUT FILE IS WRITTEN AND THE PROGRAM TERMINATES.
156      CALL HELFAS (1)
157      CALL EXIT
158      STOP
159      END

```







21	15	41	
22	15	41	
23	10	53	
24	10	53	
25	15	41	
26	15	41	
27			
28			
29			
30			
31			
32			
33			
34			
35			
36			
37			
38			
39			
40			
41			
42			
43			
44			
45			
46			
47			
48			
49			
50			
51			
52			
53			
54			
55			
56			
57			
58			
59			
60			
61			

3P	85	148	
200P	65	155	
201P	95	151	
1000P	31	32	
2000P	48	49	
2001P	46	47	
2003P	149	150	
2004P			
2005P			
2006P			
2007P			
2008P			
2009P			
2010P			
2011P			
2012P			
2013P			
2014P			
2015P			
2016P			
2017P			
2018P			
2019P			
2020P			
2021P			
2022P			
2023P			
2024P			
2025P			
2026P			
2027P			
2028P			
2029P			
2030P			
2031P			
2032P			
2033P			
2034P			
2035P			
2036P			
2037P			
2038P			
2039P			
2040P			
2041P			
2042P			
2043P			
2044P			
2045P			
2046P			
2047P			
2048P			
2049P			
2050P			
2051P			
2052P			
2053P			
2054P			
2055P			
2056P			
2057P			
2058P			
2059P			
2060P			
2061P			
2062P			
2063P			
2064P			
2065P			
2066P			
2067P			
2068P			
2069P			
2070P			
2071P			
2072P			
2073P			
2074P			
2075P			
2076P			
2077P			
2078P			
2079P			
2080P			
2081P			
2082P			
2083P			
2084P			
2085P			
2086P			
2087P			
2088P			
2089P			
2090P			
2091P			
2092P			
2093P			
2094P			
2095P			
2096P			
2097P			
2098P			
2099P			
2100P			
2101P			
2102P			
2103P			
2104P			
2105P			
2106P			
2107P			
2108P			
2109P			
2110P			
2111P			
2112P			
2113P			
2114P			
2115P			
2116P			
2117P			
2118P			
2119P			
2120P			
2121P			
2122P			
2123P			
2124P			
2125P			
2126P			
2127P			
2128P			
2129P			
2130P			
2131P			
2132P			
2133P			
2134P			
2135P			
2136P			
2137P			
2138P			
2139P			
2140P			
2141P			
2142P			
2143P			
2144P			
2145P			
2146P			
2147P			
2148P			
2149P			
2150P			
2151P			
2152P			
2153P			
2154P			
2155P			
2156P			
2157P			
2158P			
2159P			
2160P			
2161P			
2162P			
2163P			
2164P			
2165P			
2166P			
2167P			
2168P			
2169P			
2170P			
2171P			
2172P			
2173P			
2174P			
2175P			
2176P			
2177P			
2178P			
2179P			
2180P			
2181P			
2182P			
2183P			
2184P			
2185P			
2186P			
2187P			
2188P			
2189P			
2190P			
2191P			
2192P			
2193P			
2194P			
2195P			
2196P			
2197P			
2198P			
2199P			
2200P			
2201P			
2202P			
2203P			
2204P			
2205P			
2206P			
2207P			
2208P			
2209P			
2210P			
2211P			
2212P			
2213P			
2214P			
2215P			
2216P			
2217P			
2218P			
2219P			
2220P			
2221P			
2222P			
2223P			
2224P			
2225P			
2226P			
2227P			
2228P			
2229P			
2230P			
2231P			
2232P			
2233P			
2234P			
2235P			
2236P			
2237P			
2238P			
2239P			
2240P			
2241P			
2242P			
2243P			
2244P			
2245P			
2246P			
2247P			
2248P			
2249P			
2250P			
2251P			
2252P			
2253P			
2254P			
2255P			
2256P			
2257P			
2258P			
2259P			
2260P			
2261P			
2262P			
2263P			
2264P			
2265P			
2266P			
2267P			
2268P			
2269P			
2270P			
2271P			
2272P			
2273P			
2274P			
2275P			
2276P			
2277P			
2278P			
2279P			
2280P			
2281P			
2282P			
2283P			
2284P			
2285P			
2286P			
2287P			
2288P			
2289P			
2290P			
2291P			
2292P			
2293P			
2294P			
2295P			
2296P			
2297P			
2298P			
2299P			
2300P			
2301P			
2302P			
2303P			
2304P			
2305P			
2306P			
2307P			
2308P			
2309P			
2310P			
2311P			
2312P			
2313P			
2314P			
2315P			
2316P			
2317P			
2318P			
2319P			
2320P			
2321P			
2322P			
2323P			
2324P			
2325P			
2326P			
2327P			
2328P			
2329P			
2330P			









```

34 1A(UMIL-GF, SLOPE) GO TO 3
35 P41N(A2-Z21)/(X1-A2)
36 IF( P41N .LT. SLOPE) GO TO 3
37 1B( X1 .EQ. X2) GO TO 4
38 A2(Z2-Z21)/(X2-X1)
39 A2Z1-A2(X1-A2)
40 X21(A2-B)/(A-SLOPE)+A2
41 Z21A-SLOPE*(X1-A2)+A2
42
43 THIS SURPHING WILL INTEGRATE OVER THE STRIP TOP
44 C COMPLEX "RAIN" EFFECT OF THIS STRIP WILL BE ADDED TO ME ALL MI
45 C IN COMMON "VALL"
46 CALL SUM
47 SLOPEPHIL
48 CONTINUE
49 P41N
50
51
52
53
54
55
56
57
58
59
60
61
62
63
64
65
66
67
68
69
70

```

# CONSTANTS

0 201400000000

## COMMON

	PI	/REC	/GO	BY	/RFC	/S1	P2	/RFC	/S2	AX	/A1	/A2	/A3	/A4	/A5
A2		/ANT	/S2	N	/GROUND/S0		X1	/GROUND/S1		Z1	/SEG	/S1			
Z2		/GROUND/S0		IFL	/GROUND/S1		X1	/SEG	/S2	Z2					
Z22		/SEG	/S1	N	/SEG	/S1									

## SURPROGRAMS

### SUM

### SCALARS

	SCAL	143	SLOPE	144	P41N	145	AX	146	P2	147	AX	148	AX	149	AX
X1	0		Z21	1	X1	2	Z22	3	X2	4	Z21	5	Z21	6	Z21
DELX	147		AX	0	AX	2	P41N	148	AX	7	AX	8	AX	9	AX
N	142		BY	1	AX	2	AX	1	AX	10	AX	11	AX	12	AX
N	4				AX	2									

### ARRAYS

	X1	1	Z1	25	X2	51	Z2	70
--	----	---	----	----	----	----	----	----

A	58	59	60						
ANT	11	50	55	59	60	61			
AX	11	50							
AY	11								
AZ	11	52	55	60	61				
A	59	60							
DELX	50	51	52						
GROUND	12								
I	20	28	29	30	31				
TEL	12								
J	12	20							
K	13								
N	13								
PMIA	55	59							
PHIE	17	52	54	67					
REC	10								
RI	10	37	42	43	44				
RI	10								
PZ	10								
ACAF	9								
REC	13								
ALOPZ	14	53	54	56	60	61	67		
SUM	66								
X1	12	28							
X2	12	30							
X3	13	28	37	42	55	57	58	60	61
X4	13	30	42	43	44	50	57		
X5	13	29							
X6	12								
X7	12	31							
X8	13	29	43	55	58	59	61		
X9	13	31	43	52	58				
X10	13								

1P	20	54							
3P	51	53	60						
4P	57	61							
5P	42	45							
6P	37	60							



```

54  NXL1
55  LTOU
56  C
57  C THESE ARE THE LIMITS AND UPPER BOUNDS FOR THE SPACING METHOD
58  C POINTS ALONG THE VARIABLE OF INTEGRATION
59  L33 LAMBDA/24.
60  L10020.0LAMBDA
61  ALPH1=11
62  A2=121
63  B1=11
64  B2=11-A2
65  A=11
66  TEMP=12
67  AS=12
68  AS=12
69  AS=12
70  AS=12
71  AS=12
72  AS=12
73  AS=12
74  AS=12
75  AS=12
76  AS=12
77  AS=12
78  AS=12
79  AS=12
80  AS=12
81  AS=12
82  AS=12
83  AS=12
84  AS=12
85  AS=12
86  AS=12
87  AS=12
88  AS=12
89  AS=12
90  AS=12
91  AS=12
92  AS=12
93  AS=12
94  AS=12
95  AS=12
96  AS=12
97  AS=12
98  AS=12
99  AS=12
100  AS=12
101  AS=12
102  AS=12
103  AS=12
104  AS=12
105  AS=12
106  AS=12

```







JNI PT	1142 1	N	4	MM	U	MI	I	AA			
A	65	67	71	74	80	87	115	117	121	131	154
A1	26	61	65	81	47	111	115	132	154		
A2	26	82	66	87	112	116	154				
AS	92	154									
AK	29	30	37	74	124						
AKK	37	42	135								
AMT	30										
AP	87	92	154	158							
AL	30										
AV	30	36	72	122							
AS2	26	36									
A2	30	64	179								
B	68	70	71	74	80	84	118	120	121	141	154
B1	26	63	68	84	113	114	155				
B2	26	64	69	88	114	119	155				
BP	88	92	155	158							
C	73	77	78	79	80	92	123	124	130	131	154
CE	34	42	47	87	88	110	154	155	174		
CF	83	85	86	136	141	144					
CO6	83	136									
D	78	81	82	129	132	135					
DALE	36	72	76	122	128						
DL	95	96	97	98	109	110	145	161	162	164	170
DICE	110	111	113								
DLAE	100	112	114								
DPI	24	30	75	76	125	124					
DR	28	72	73	74	75	76					
DSORT	72	122									
F	76	83	84	129	136	137					
FLOAT	76	120									
EP	92	95	158	161	132	175	141	144			
G	61	82	85	86							
HL	32	181									
HR	32	180									
I	75	76	125	126							
IL	95	151	172								
JL	27	49	150	181							
JMI	27	144	150	153							
JMR	23	141	149	152							
JOI	27	86	150	153							
JOR	27	85	149	152							
JR	27	48	148	180							
LLO	33	60	98	162							
LS	33	54	95	97							
LAORDA	28	30	59	60							
N	25	178									
RI	54	164	178								
R	70	61	130	132							
REC	31										
RI	31	61									
RZ	31										
RZ	31	62									
S	80	81	131	132							

PC	38	42	46	87	88	109	154	155	179								
SEC	25																
ST	84	85	86	137	141	144											
SIN	84	137															
APCL	37	123															
CONT	42	67	70	80	117	120	131										
SW	24																
TEMP	66	67	69	70	71	72	77	87	85								
	121	122	123	135	141	144	145	149	150								
VAL	32	39	61	63	179												
X1	25	39															
X2	25	39															
KL	26	53	98	168	169	170	171										
MAX	42	46	47	169	170	171											
LI	25	38	62	64	179												
Z2	25	38															

1P	103	169	173
2P	151	177	

1 2 3 4 5 6 7 8 9 10 11 12 13 14 15 16 17 18 19 20 21 22 23 24 25 26 27 28 29 30 31 32 33 34 35 36 37 38 39 40 41 42 43 44 45 46 47 48 49 50 51 52 53

46





49





```

1 SUBROUTINE NORMAL(V1,V2,V3,V4,M)
2 DIMENSION V1(1),V2(1),V3(1),V4(1)
3 X1=V2(1)-V1(1)
4 X2=V3(1)-V1(1)
5 X3=V4(1)-V1(1)
6 Y1=V2(2)-V1(2)
7 Y2=V3(2)-V1(2)
8 Y3=V4(2)-V1(2)
9 Z1=V2(3)-V1(3)
10 Z2=V3(3)-V1(3)
11 Z3=V4(3)-V1(3)
12 P=SQRT(X1**2+X2**2+X3**2)
13 V1(1)=V1(1)+X1/P
14 V1(2)=V1(2)+X2/P
15 V1(3)=V1(3)+X3/P
16 P=SQRT(Y1**2+Y2**2+Y3**2)
17 V1(2)=V1(2)+Y1/P
18 V1(3)=V1(3)+Y2/P
19 P=SQRT(Z1**2+Z2**2+Z3**2)
20 V1(3)=V1(3)+Z1/P
21 V1(4)=V1(4)+Z2/P
22 V1(5)=V1(5)+Z3/P
23 RETURN
24 END

```

# GLOBAL DIMENSIONS

V1	133	V2	134	V3	135	V4	136	M	137
----	-----	----	-----	----	-----	----	-----	---	-----

## SUBPROGRAMS

### SORT

### SCALARS

NORMAL	101	X1	102	X2	103	V1	104	V2	105	V3	106	V4	107	M	108
X1	109	X2	110	X3	111	Y1	112	Y2	113	Y3	114	Z1	115	Z2	116
P	117														

### ARRAYS

V1	13	V2	134	V3	135	V4	136
----	----	----	-----	----	-----	----	-----

NORMAL	1	12	13	14	15	16	17	18	19	20	21	22
P	1	2	3	4	5	6	7	8	9	10	11	12
X1	1	2	3	4	5	6	7	8	9	10	11	12
X2	1	2	3	4	5	6	7	8	9	10	11	12
X3	1	2	3	4	5	6	7	8	9	10	11	12
Y1	1	2	3	4	5	6	7	8	9	10	11	12
Y2	1	2	3	4	5	6	7	8	9	10	11	12
Y3	1	2	3	4	5	6	7	8	9	10	11	12
Z1	1	2	3	4	5	6	7	8	9	10	11	12
Z2	1	2	3	4	5	6	7	8	9	10	11	12
Z3	1	2	3	4	5	6	7	8	9	10	11	12
P	1	2	3	4	5	6	7	8	9	10	11	12

```

1  DOUBLE PRECISION FUNCTION DIST(X,Y)
2  DIMENSION X(1),Y(1)
3  DOUBLE PRECISION P,TEMP
4  REAL
5  NO 1 (M1,3)
6  TEMP=X(1)-Y(1)
7  TEMP=TEMP*TEMP
8  DIST=DSORT(N)
9  RETURN
10 END

```

CLIMAT, DIMMITS

X 56 Y 57

SUBPROGRAMS

NO 2 DIM-2 DSORT

SCALARS

DIST 60 P 62

ARRAYS

X 56 Y 57

TEMP 65

N4

1

DIST	1	4
DSORT	4	6
X	5	4
Y	3	7
TEMP	1	2
P	1	6

1P 5 7

# PROGRAM INT2.F4

```

1 SUBROUTINE INT2(CTEMP)
2 DATA DI,DY/23,40,
3 DIMENSION XTA(3),ZTA(3)
4 DOUBLE PRECISION D10,D20,A10,M20
5 COMPLEX A,M
6 DOUBLE PRECISION DR1,DR2
7 COMPLEX CTEMP,CCT,CCX,CCY,CCXU
8 REAL LAMBDA,M1,M2,M3
9 COMMON /CAND/ P(3,4),M(3)
10 EQUIVALENCE (M(1),M1),M(2),M2),M(3),M3)
11 DOUBLE PRECISION DAK-DP1
12 COMMON /REC/ R,XP,ZP
13 COMMON /INT/ XA,TA,ZA,LAMBDA,DAK-DP1
14 EQUIVALENCE (P1,P(1,1)),P(2,P(1,2)),P(3,P(2,1))
15 EQUIVALENCE (P2,P(2,4)),P(3,P(3,1)),P(3,P(3,4))
16 LOGICAL TEST
17 DATA TEST/.TRUE./
18 IF (TEST) CALL NORMAL(P1,P2,P(1,3),P(1,4),P(1,5),TEMP)
19 TEST=.FALSE.
20 ZA=2.2*ZA
21 TP1=SMGL(DP1)
22 AS=SMGL(DAK)
23 CTEMP=(0.,0.)
24 DELZ=DP1
25 DGO=INT(D(1,1),D(1,2))
26 IXC=0/DELX
27 IF (IX .LT. 0) IX=-IX
28 IF (IX .LT. 1) IX=1
29 IXC=((IX+1)/2)*2
30 DELX=DCO/FLOAT(IX)
31 XTA(1)=P(1,2)-P(1,1)/DCO
32 XTA(2)=P(2,2)-P(2,1)/DCO
33 XTA(3)=P(3,2)-P(3,1)/DCO
34 DGO=XTA(1)*DELX
35 DGO=XTA(2)*DELX
36 DGO=XTA(3)*DELX
37 DC1=DIST(P(1,1),P(1,4))
38 DELZ=DPY
39 IZ=DC1/DELZ
40 IF (IZ .LT. 0) IZ=-IZ
41 IF (IZ .LT. 1) IZ=1
42 IZ=((IZ+1)/2)*2
43 DELZ=DC1/FLOAT(IZ)
44 ZTA(1)=P(1,4)-P(1,1)/DC1
45 ZTA(2)=P(2,4)-P(2,1)/DC1
46 ZTA(3)=P(3,4)-P(3,1)/DC1
47 DGI=ZTA(1)*DELZ
48 DGI=ZTA(2)*DELZ
49 DGI=ZTA(3)*DELZ
50 DO IXX=1,IX
51 FX=FLOAT(IXX)-5
52 XSP(1,1)=FX*DCGX
53 YSP(2,1)=FX*DCGY

```

54	ZAMP(3,1)*FONGH2
55	IN 2 122*1,12
56	FZPLNAT(122)*.5
57	ZSXS*FZDGIK
58	YSYS*FZDGIK
59	ZSXS*FZDGIK
60	CC*YS-XS
61	CC*YS-XS
62	TEMP*YS
63	TEMP*YS-XS
64	TEMP*YS-XS
65	TEMP*YS-XS
66	DM1*DMLE(C*CC*CC)*DMLE(TEMP*TEMP)
67	DM2*DM1*DMLE(TEMP*TEMP)
68	DM1*DM1*DMLE(TEMP*TEMP)
69	R22*DM2
70	R10*DM2*DM1
71	R20*DM2*DM1
72	R1*DM1
73	R2*DM2
74	TEMP*YS-XS
75	TEMP*YS-XS
76	TEMP*YS-XS
77	DM1*DMLE(C*CC*CC)*DMLE(TEMP*TEMP)
78	DM2*DM1*DMLE(TEMP*TEMP)
79	DM1*DM1*DMLE(TEMP*TEMP)
80	R22*DM2
81	R10*DM2*DM1
82	R20*DM2*DM1
83	R1*DM1
84	R2*DM2
85	F10*DM2*YS*(YS-YS)*(M1*YS*3*(ZS-ZA))*((M1*YS)
86	F20*DM2*YS*(YS-YS)*3*(ZS-ZA)
87	C08A*(YS*(1)*CC*YS*(2)*((YS-YS)*YS*(3)*((ZS-ZA))/D1
88	C08A*(YS*(1)*CC*YS*(2)*((YS-YS)*YS*(3)*((ZS-ZA))/D2
89	C08A*(YS*(1)*CC*YS*(2)*((YS-YS)*YS*(3)*((ZS-ZA))/D1
90	C08A*(YS*(1)*CC*YS*(2)*((YS-YS)*YS*(3)*((ZS-ZA))/D2
91	C08A*(YS*(1)*CC*YS*(2)*((YS-YS)*YS*(3)*((ZS-ZA))/D1
92	C08A*(YS*(1)*CC*YS*(2)*((YS-YS)*YS*(3)*((ZS-ZA))/D2
93	C08A*(YS*(1)*CC*YS*(2)*((YS-YS)*YS*(3)*((ZS-ZA))/D1
94	C08A*(YS*(1)*CC*YS*(2)*((YS-YS)*YS*(3)*((ZS-ZA))/D2
95	C08A*(YS*(1)*CC*YS*(2)*((YS-YS)*YS*(3)*((ZS-ZA))/D1
96	C08A*(YS*(1)*CC*YS*(2)*((YS-YS)*YS*(3)*((ZS-ZA))/D2
97	C08A*(YS*(1)*CC*YS*(2)*((YS-YS)*YS*(3)*((ZS-ZA))/D1
98	C08A*(YS*(1)*CC*YS*(2)*((YS-YS)*YS*(3)*((ZS-ZA))/D2
99	C08A*(YS*(1)*CC*YS*(2)*((YS-YS)*YS*(3)*((ZS-ZA))/D1
100	C08A*(YS*(1)*CC*YS*(2)*((YS-YS)*YS*(3)*((ZS-ZA))/D2
101	C08A*(YS*(1)*CC*YS*(2)*((YS-YS)*YS*(3)*((ZS-ZA))/D1
102	C08A*(YS*(1)*CC*YS*(2)*((YS-YS)*YS*(3)*((ZS-ZA))/D2
103	C08A*(YS*(1)*CC*YS*(2)*((YS-YS)*YS*(3)*((ZS-ZA))/D1
104	C08A*(YS*(1)*CC*YS*(2)*((YS-YS)*YS*(3)*((ZS-ZA))/D2
105	C08A*(YS*(1)*CC*YS*(2)*((YS-YS)*YS*(3)*((ZS-ZA))/D1
106	C08A*(YS*(1)*CC*YS*(2)*((YS-YS)*YS*(3)*((ZS-ZA))/D2

```

107 PZER20QUAK
108 ID=10/DPI
109 D1=10-DLE(FLOAT(10))@DPI
110 ID=20/DPI
111 D2=20-D1F(FLOAT(10))@DPI
112 ID=10/DPI
113 D1=10-D1F(FLOAT(10))@DPI
114 ID=20/DPI
115 D2=20-D1F(FLOAT(10))@DPI
116 TEMPEF10=10SIN(ARCCOS(DELX*.5)*SIN(ARCCOS(17*.5)/(CHOC(12+12))
117 CTEMP=CTMP+TFP@CEXP(CMPLX(0.,01+M1))
118 TEMPEF10=10SIN(ARCCOS(DELX*.5)*SIN(ARCCOS(12*.5)/(CHOC(12+12))
119 CTEMP=CTEMP+TFP@CEXP(CMPLX(0.,01+M2))
120 TEMPEF20=10SIN(ARCCOS(DELX*.5)*SIN(ARCCOS(20*.5)/(CHOC(20+22))
121 CTEMP=CTEMP+TFP@CEXP(CMPLX(0.,02+M1))
122 TEMPEF20=10SIN(ARCCOS(DELX*.5)*SIN(ARCCOS(20*.5)/(CHOC(20+22))
123 CTEMP=CTEMP+TFP@CEXP(CMPLX(0.,02+M2))
124 CONTINUE
125 2
126 CTEMP=CTEMP*2./(TPI@TPI)
127 ICC=IX*12
128 RETURN
129 END

```

CONSTANTS

	0	000000000000	1	000000000000	2	000000000001	3	000000000000
GLOBAL DIMMELS								
CTEMP	1341							
COMMON								
P	/GRND /+0	N	/GRND /+14	XN	/R/C /+0	YN	/R/C /+1	ZM
XA	/ANT /+0	YA	/ANT /+1	ZA	/ANT /+2	LA@MDA	/ANT /+3	LA
DPI	/+6	M1	/GRND /+14	N2	/GRND /+15	M3	/GRND /+16	PI1
PI2	/GRND /+3	P21	/GRND /+1	P24	/GRND /+12	P11	/GRND /+3	P31
SUBPROGRAMS								
NORMAL	SNGL	DIST	D	IFIX	FLUAT	USKRT	IFX	IFX
SIM	CEXP	CMPLX	CFM*.0	CFD*.4				
SCALARS								
TNTR2	1347	DX	1350	DY	1351	TEST	1352	PI1
PI2	3	TEMP	1353	ZA2	1354	ZA	2	IP1
DPI	6	AK	1356	DAA	4	CTF SP	1361	CTF A
DGO	1360	TX	1361	UGOR	1362	USG1	1363	UGO2
DC1	1365	DELZ	1366	I2	1367	UG14	1370	UG1
DC1Z	1372	YXX	1373	FX	1374	X5	1375	VS
Z5	1377	I22	1400	FZ	1401	CCN	1402	XM





58



95	44	45	46	47	48	49	92	93	94	95
3										

1P	50	125
2P	55	124

```

DIMENSION ILABL(PI)
COMMON /PLUT/ WP,PRX,WRX,X,LM,ML,I,DELTA,MY,MZ,MYX,MYX1,MYZ1,
1ZM2,2MX,2MZ,2Z1,2MY,2MY1,2MYX,2MYX1,2MYZ,
2ZM2,2MX,2MZ,2Z1,2MY,2MY1,2MYX,2MYX1,2MYZ,
3AD1X,AD1Z,AD1Y,AD1X,AD1Y,AD1Z,
4AD1X,AD1Z,AD1Y,AD1X,AD1Y,AD1Z,
FUNITALENCE (IPIPIAT(1),WRP)
IMPLICIT COMPLEX (C)
DIMENSION X(20),Y(20),Z(20)
DIMENSION CF1(20),CF2(20),CF3(20)
IMPLICIT DOUBLE PRECISION (D)
COMMON /REC/IX,IY,IZ,MY,MZ,NT,NSIZ
REAL LAMBDA
COMMON /GRUND/ K,X(20),Z(20),XZ(10),ZZ(10),Y(10),
COMMON /MY/AX,AY,AZ,LANRPA,LAN,PP1
COMMON /VAL/ WP,MI

C THIS VALUE OF TAO PI IS INITIALIZED THIS WAY TO AVOID L(S)
C
C BLOCK DATA
DPI=6.2831853071795864769
WRITE(5,2001)
2001 FORMAT(' INPUT FILE NAME:',*8)
2000 READ(5,2000) ILBL
2000 FORMAT(I5)
CALL IFILE(20,ILBL)
WRITE(5,2002)
2002 FORMAT(' OUTPUT FILE NAME:',*8)
READ(5,2000) ILBL
CALL OFILE(1,ILBL)
WRITE(1) IPIAT
READ(20,1000) ILABL,TAU
WRITE(1,1000) ILABL
DO 3 I=1,2
READ(20,1000) ILABL
WRITE(1,1000) ILABL
FORMAT(85,F)
3 READ(20) LAMBDA,ML,(X(1),Y(1),Z(1),CF1(1),CF2(1),CF3(1),
1CFR1,CFR2,CFR3,CFR1,CFR2,CFR3)
201 READ(20,2005) NSIZ,MY,MZ,NT,
1CFR1,CFR2,CFR3,CFR1,CFR2,CFR3)
2005 FORMAT(4F,7.6F13.6,7.6F13.6)
C
C AFTER THE FIELDS HAVE BEEN ACCUMULATED FOR ALL THE FIELDS
C
C THE CDI'S ARE CALCULATED
C
C ACDC CDI FOR THE GROUND SURFACE
C
C ACDC CDI FOR 'IDEAL' GROUND PLANT
C
C ACDC=57.14*MFAL((CFR2-CFR3)/CFR1)
C
C ACDC=57.14*MFAL((CFR2-CFR3)/CFR1)
C
C MCRP IS THE COUNT OF THE RECEIVERPRINTS
C
C MCRP=PI
C
C IF(MP.NE. 1) GO TO 4

```











```

1 DIMENSION TYPE(3,2)
2 DATA TYPE/STAT/,C VAL*,'T'S',('I'NA**,'IC VAS','I'US**/'
3 DATA FID,PBD/'CDI*', 'THRON',
4 DIMENSION SPACE(4),LX(2,3)
5 DATA SPACE/1.,2.,2.5,5./
6 DATA LAX/'DEGRE', 'ES', 'EFTT',
7 DATA PRY,PRZ,PRT,PAL,PAF/
8 'M', 'R', 'H2', 'HT', 'CDI', 'THN0'/
9 DIMENSION IPTDAT(33)
10 COMMON /PIRMGRP,PARM,RK,X,PRD,T,FIL,T,PM,N,MV,Z,PH,T,VIT,
11 IZMI,IEXM,PZF,T,WZLT,PTMM,MIX,X,EFT,MTUL,
12 JAIM,IEXM,AIFT,ALT,APMX,AMTX,AMT,AMUT,
13 VAL I,ADIX,ADIF,ADIL,ADR*,APRX,AMPX,ADWL
14 EQUIVALENCE (IPTDAT(1),NM*)
15 DIMENSION PLAN(R)
16 DATA BLFN,YLFN,ITIC/20.,8.,.21/
17 DIMENSION NYI(2000)
18 DIMENSION DX(2000),DY(2000)
19 NAMELIST FMED/YLFNG,YDFI,YSC,DUMIN,DVAX,DPFL,C,FSC
20 CALL PLOTSCIRIM,160,63)
21 WRITE(5,1006)
22 FORMAT(' INPUT FILE NAME AND AXIS TYPES:',*)
23 HEAD(5,1006) NAME,ISX,ISY,MUIND
24 FORWAT(AS,I,I,I)
25 IF(ISX .LT. 1) GO TO 204
26 IF(ISY .GT. 2) GO TO 204
27 IF(ISX .LT. 1) GO TO 204
28 IF(ISY .GT. 3) GO TO 204
29 CALL PLOT(0.,-12.,-3)
30 CALL PLOT(0.,1.,-3)
31 I=0
32 CALL IFILE(20,NPMT)
33 PFAL(20) IPTDAT
34 WRITE(3,1002) NMP
35 FORMAT(' THERE ARE ',IS,' RECTIVER POINTS.',/)
36
37
38
39
40
41
42
43
44
45
46
47
48
49
50
51
52
53
54
55
56
57
58
59
60
61
62
63
64
65
66
67
68
69
70
71
72
73
74
75
76
77
78
79
80
81
82
83
84
85
86
87
88
89
90
91
92
93
94
95
96
97
98
99
100
101
102
103
104
105
106
107
108
109
110
111
112
113
114
115
116
117
118
119
120
121
122
123
124
125
126
127
128
129
130
131
132
133
134
135
136
137
138
139
140
141
142
143
144
145
146
147
148
149
150
151
152
153
154
155
156
157
158
159
160
161
162
163
164
165
166
167
168
169
170
171
172
173
174
175
176
177
178
179
180
181
182
183
184
185
186
187
188
189
190
191
192
193
194
195
196
197
198
199
200

```



54	100	FORMAT(AS)
55		CALL SYMBOL(0,0,0,2,ILANL,90,0,40)
56	7	CALL PRINT(,3,0,0,3)
57		CALL SYMBOL(0,0,0,2,ITIP(1,ISY),90,15)
58		CALL PLOT(2,0,0,3)
59	1	READ(20,1000,END=2) X,Y,Z,T,C,W,CD,M0
60	1000	FORMAT(F)
61		Y=MSORT(X*Y)
62		IF((TEMP.LT. 1500.) .OR. (TEMP.GT. 20720.)) GO TO 60
63		GASUGASUC
64		GASUGASUCD
65	60	GASUGASUC+1.
66		CONTINUE
67		ISL=.
68		GO TO (300,301) ISY
69	300	CONTINUE
70		DX(1)=C
71		DX(1)=R
72		GO TO 302
73	301	DX(1)=CD
74		DX(1)=RD
75	302	CONTINUE
76		GO TO (200,201,202) ISK
77	200	DX(1)=ATAN2(Z,SURT(X*Y))\$57.2953
78		GO TO 199
79	201	DX(1)=X
80		GO TO 199
81	202	DX(1)=Y
82		GO TO 199
83	199	IF(1.-MX. 1) GO TO 198
84		DMIN=DX(1)
85		DMAX=DX(1)
86	198	DMIN=MIN(DMIN,DX(1))
87		DMAX=MAX(DMAX,DX(1))
88	1001	FORMAT(SX,IF)
89		IF( 1 .LT. 2000) GO TO 1
90	2	IF(1 .LT. 2) GO TO 3
91		YLENG=MAX(1,MIN,ABS(ROUND),-AIM,6.)
92		IF(ABS(ROUND) .LT. 1.E-4) GO TO 10
93		YDEL=YLENG
94		GO TO 11
95	10	YLENG=MAX(1,YLENG,ABSX,-APMN)
96		YOF=FLOAT(FIX(YLENG/YLNM))
97		YLENG=YDEL*YLEN
98	11	CALL AXIS(0,0,0,-YLENG,YLENG,YDEL,YLEN,
99		1'MICROAMPERS',12,0,0,0,YSC)
100		IP=FIX(ALOG10(DMAX-DMIN))-1
101		POM=10.**IP
102		DO 120 J=1,4
103		DEL=SPACE(J)*POM
104		IT=FIX(DMAX/DEL-1)+1-IFIX(DMIN/DFL)
105		IF(IT.LT. 1)IC GO TO 121
106	120	CONTINUE





70

J	102	103	122	123	124	124	127	127	127	131	131	134
NAME	23	32										
MRP	10	14	34									
PAI	7	43										
PAR	7	44										
PLO	3	45										
PLDI	29	30	56	58	112	113	115	124				
PLOTS	20											
PUN	101	103										
PUN	3	46										
PRI	7	42										
PRK	7	39										
PRY	7	40										
PRZ	7	41										
PXIN	10	71										
R	54	74										
RD	59	74										
RFT	10	42										
RILT	10	42										
RYNN	10	42										
RZML	10	42										
RFT	10	39										
RILT	10	39										
RYNN	10	39										
RFT	10	40										
RILT	10	40										
RYNN	10	40										
RFT	10	41										
RILT	10	41										
RYNN	10	41										
RZML	10	41										
SPACE	4	5	103									
SGRT	61	77										
SYMBOL	55	57										
I	59	81										
TEMP	61	62										
X	52	61	77	79								
XLW	16	111	113	131								
YSC	19	111	115	124	127	129						
Y	59	61	77									
YDEL	19	93	96	97	98							
YLEN	16	96	97	98	112							
YLENG	10	91	93	95	96	97	98					
YSC	10	98	115	124	127	129						
Z	59	77										

1P 59 89  
 2P 59 90  
 3P 21 122  
 4P 122 124  
 5P 128 130  
 6P 50 56  
 7P 125 131  
 8P 92 95  
 9P 24 98  
 10P 62 66  
 11P 51 54  
 12P 52 53  
 13P 102 106  
 14P 104 107  
 15P 83 86  
 16P 76 80  
 17P 76 77  
 18P 76 79  
 19P 76 81  
 20P 25 26  
 21P 68 69  
 22P 73 75  
 23P 60 62  
 24P 116 119  
 25P 34 35  
 26P 37 39  
 27P 38 40  
 28P 23 24  
 29P 21 22  
 30P 119 120

```

1 SUBROUTINE AXIS(X0,Y0,AXX,ANY,DXLA,AINCH,NCU,CL,NIFC,LAB,PI)
2 DIMENSION RCU(1)
3 HT = .16
4 DELX=SIGN(DELX,(AXX-AMIN))
5 W1=0.
6 W2=0.
7 W3 = 0.
8 *KX = 0
9 NCHEARS(NCH)
10 IF(PH,AT,0.) *KX = 0
11 CINCHEARS(AINCH)
12 IF(ARS(AMX-AMIN)*ARS(DELA),IT,1,3) GO TO 40
13 IF((ARS-AMIN)/(DFLX+1,5),CT,3,5) CINCHEARS(AMX-AMIN)/(1,5)
14 IF(NCH,LT,0) W3 = 1.
15 NHEARS(IT,(AMX-AMIN)/DFLX+1,4)
16 ANCH=CINCHEARS/FLUAT(MIN=1)
17 IF(AINCH,LT,0) GO TO 5
18 *ZEL.
19 GO TO 10
20 5 W1=1.
21 10 CALL PLOT(X0,Y0,3)
22 DELX=FLX/10,00000/ANC
23 ANCH=AMIN-DELA
24 X=0.
25 Y=0.
26 XW=0.
27 YW=0.
28 DU 40 101,NUM
29 ANCH=ANP*DELA
30 I1=0
31 I2=11+1
32 25 IF(ARS(ANUM)/10,001,1,1,3) GO TO 20
33 I2=I1+1
34 GO TO 25
35 20 IF(ANUM,LT,0) I2=I1+1
36 IF(ARS(ANUM),1,1,1) I2=I1+1
37 IWOFE=NDFC+1
38 I1=I1+IMORE
39 IF(I1,IMORE)
40 IF(I1,IMORE)
41 HT = ANCH/HT,ANC/FLUAT(I1+2)
42 CENTER = FLUAT(I1)HT/(1,0+1)
43 OFF = .05
44 XC = X - CENTER + *2*(W3*(30+CINCH)) - .15)
45 IF(XC,LT,XMIN) XC
46 YC = Y - *1*(HT + .15 - W3*(HT+3)) - *2*OFF
47 CALL PLOT(X0,X,Y,2)
48 CALL PLOT(X0,X,10+2,Y,10+3)
49 CALL PLOT(X0,X,-10+2,Y,-10+3)
50 CALL NUMBER(X0,X,Y,ANC,HT,ANUM,0,NDFC)
51 CALL PLOT(X0,X,Y,1,3)
52 X=X+ANCO*1
53 Y=Y+ANCO*2
54 40 CONTINUE
55 RST = (CINCHEARS - FLUAT(NCH+NEAR)*.12)/2.
56 XIC = W1*(X0 + HST) + W2*(X0 + XW - OFF) + W3*(2,0,CINCH,44)
57 YIC = W1*(Y0 + YC - .17 + W3*(HT + .22)) + W2*(Y0 + HST)

```

```

54 CALL SYMVAL (KX,YC,12,NO,90,002,ACH)
55 IF (P, EQ, 0) RETURN
56 CALL MEMP (XU,YU,XCX)
57 CALL SYMVAL (XU,YU,12,NO,10,90,002,5)
58 CALL MEMP (XU,YU,XCX)
59 X = XU + (XCX,00-XC)002
60 Y = YU + (YC,00-YC)001
61 CALL NUMPR (X,Y,09,00,90,002,0-1)
62 RETURN
63 50 DELC = 1.5-3010.00PR/CINCH
64 NCHC/Y
65 WRITE (5,1000) AMX,AMIN,DELA,PM, (RCO(1),10,1)
66 1000 FORMAT (10,27INSUFFICIENT RANGE FOR AXIS,
67 1/1X,4G,7,1X,13A)
68 CALL EXIT
69 RETURN
70 END

```

CONSTANTS

	0	1	2	3	4
0	175611463146	167406111564	100517426542	201130311041	4
1	201400000000	174631463146	177461146314	178461146314	11
2	000000000000	175753412172	177702436560	178534121721	16
3	201244030540	000000000000	000000000005	175507531121	21

GLOBAL VARIABLES

	X0	Y0	ACH	AMX	AMIN	DELA	PM	RCO(1)	RCO(2)
X0	656			656	656				
ACH	663			664	664				
DELA	670								

SUBPROGRAMS

	SIGN	IARS	ABS	FIX	PLUT	EXP2.7	EXP2.2	APL	APL	APL
SIGN	673			674						
IARS	661			676						
ABS	702			665						
FIX	704			705						
PLUT	706			707						
EXP2.7	713			714						
EXP2.2	717			720						
APL	724			725						

SCALARS

	AXIS3	AMIN	NCH	NUM	II	XC	XO	APAYS	BCD
AXIS3	673								
AMIN	661								
NCH	702								
NUM	704								
II	713								
XC	717								
XO	724								
APAYS	664								
BCD	664								



75

5P	20
10P	21
20P	33
25P	32
30P	30
40P	27
50P	12
100P	65